2012-04-18

A WANFIS Model for Use in System Identification and Structural Control of Civil Engineering Structures

Ryan Mitchell
Worcester Polytechnic Institute

A WANFIS MODEL FOR USE IN SYSTEM IDENTIFICATION AND STRUCTURAL CONTROL OF CIVIL ENGINEERING STRUCTURES

by

Ryan Mitchell

A Thesis

Submitted to the Faculty

of the

WORCESTER POLYTECHNIC INSTITUTE

in partial fulfillment of the requirements for the

Degree of Master of Science

in

Civil Engineering

May 2012

APPROVED:

Dr. Yeesock Kim, Thesis Advisor

Dr. Tahar El-Korchi, Major Advisor and Head of Department

Dr. Leonard Albano, Committee Member

A WANFIS MODEL FOR USE IN SYSTEM IDENTIFICATION AND STRUCTURAL CONTROL OF CIVIL ENGINEERING STRUCTURES

by

Ryan Mitchell

A Thesis

Submitted to the Faculty

of the

WORCESTER POLYTECHNIC INSTITUTE

in partial fulfillment of the requirements for the

Degree of Master of Science

in

Civil Engineering

May 2012

APPROVED:

_____

Dr. Yeesock Kim, Thesis Advisor

_____

Dr. Tahar El-Korchi, Major Advisor and Head of Department

_____

Dr. Leonard Albano, Committee Member

Abstract

With the increased deterioration of infrastructure in this country, it has become important to find ways to maintain the strength and integrity of a structure over its design life. Being able to control the amount a structure displaces or vibrates during a seismic event, as well as being able to model this nonlinear behavior, provides a new challenge for structural engineers. This research proposes a wavelet-based adaptive neuro-fuzzy inference system for use in system identification and structural control of civil engineering structures. This algorithm combines aspects of fuzzy logic theory, neural networks, and wavelet transforms to create a new system that effectively reduces the number of sensors needed in a structure to capture its seismic response and the amount of computation time needed to model its nonlinear behavior. The algorithm has been tested for structural control using a three-story building equipped with a magnetorheological damper for system identification, an eight-story building, and a benchmark highway bridge. Each of these examples has been tested using a variety of earthquakes, including the El-Centro, Kobe, Hachinohe, Northridge, and other seismic events.

Acknowledgements

I would like to thank my thesis advisor Dr. Yeesock Kim for all his help, support, and guidance throughout the last two years of conducting research. I would also like to thank my committee members Dr. Tahar El-Korchi and Dr. Leonard Albano for their guidance and support, as well.

I would also like to thank the rest of the faculty and my friends at Worcester Polytechnic Institute for allowing me to have a great experience.

Lastly, I would like to thank my parents, Paul and Helen Mitchell, for their continued support over the last 23 years. I wouldn't have been able to accomplish all that I have without their support and advice.

Table of Contents

List of Tables

Number *Page*

List of Figures

Number *Page*

1. Overview

Structural health monitoring is a growing aspect of structural engineering that allows for the determination of the status of a structure's strength and stiffness capabilities. This is a growing and important field in structural engineering due to its ability to understand and assess the state of a structure, including assessing out the amount of damage it has sustained, or exploring strategies to control structural responses to limit damage or prevent collapse. The research outlined in the following thesis presents a new algorithm that can be used for structural control and system identification. The algorithm, a wavelet-based, adaptive neuro-fuzzy inference system, combines aspects of neural networks, fuzzy logic theory, and wavelet transforms to create a methodology that is new to the application of civil engineering structures. Using this methodology reduces the number of sensors required, computation times, and improves performances over previous systems.

System identification and structural control are important aspects in structural health monitoring. The purpose of system identification is to model the non-linear behavior of a structure when it is equipped with a control device. When a control device is installed on a structure, the behavior becomes non-linear due to the interaction effects between the device and structure. System identification eliminates the need for the development of a finite element model. This is because system identification predicts the behavior of the structure, which is something that is determined through the finite element modeling of a structure. Therefore, having an effective method for system identification allows for the bypassing of the development of the model. Structural control deals with improving the structural performance of a building or bridge by implementing control devices such as dampers and actuators to develop forces in the structure to counteract external forces, such as earthquakes. This is essential, as being able to

limit the responses of a structure can maintain the strength and integrity of the building or bridge, allowing for a safer structure over the course of the design life.

This thesis combines three journal papers that are in submission to publishers. The first paper outlines the effectiveness of the WANFIS system as a means for system identification of a building employing a smart damper. The second paper details the use of the WANFIS model as a control algorithm to improve the structural performance of a building with both active and hybrid control systems. The third paper demonstrates the WANFIS model as a control algorithm to improve the structural performance of a benchmark highway bridge using an active control system.

2. System identification of smart structures using a wavelet neuro-fuzzy model[1]

2.1. Introduction

In recent years, smart control strategies have attracted a great deal of attention from the structural engineering. However, a difficult problem in dealing with smart structures and structural health monitoring is creating an effective model of a nonlinear dynamic structure. Nonlinear systems occur when actuators and dampers, such as the magnetorheological (MR) dampers, are implemented into a structure to aid in the building's ability to withstand destructive environmental forces such as strong winds and earthquake loads. Being able to mathematically model the structure and its corresponding nonlinear dampers is a challenging task in smart control. It is generally known that the smart system produces a nonlinear behavior due to the nonlinear damper devices that a structure is equipped with, even though the structure itself is typically assumed to behave linearly, as noted by Kim et al (2009). Therefore, the challenge is to create a mathematical model to develop a relationship between the input and output of a structure that uses a nonlinear damping device. This paper proposes a new nonlinear system identification for describing nonlinear behavior of a seismically excited building equipped with smart dampers.

System identification (SI) is essential in smart structures to create a mathematical model from actual dynamic data. The goals of an effective SI is to reliably predict how a system will behave under a variety of dynamic loading scenarios such as far- and near-field earthquakes, as well as showing interactions between the system inputs and outputs. SI can be separated into two categories: parametric and nonparametric approaches, according to Adeli and Kim (2000). The parametric method identifies the structural properties of the system, including stiffness and damping systems that are intrinsically imbedded in the structure and its materials (Jalili-Kharaajoo 2004). The nonparametric method of SI is

[1] This paper is currently in review for publication in the *Journal of Smart Materials and Structures*

used to train data to the input-output map of the system (Filev 1991). This nonparametric approach is useful to SI to bridge the gap between the linear and nonlinear parts of the system. This has successfully been done with neural networks as well as fuzzy logic systems. Furthermore, the incorporation of the two systems provides a better learning model to use for SI.

The first system that is commonly used as a nonparametric method, a fuzzy inference system, uses fuzzy set theory to create a set of rules with which the system must follow. It is effective in showing the complexities that arise from nonlinearities and dynamic system uncertainties, described by Gu and Oyadiji (2008). Since the early work done by Zadeh (1965), fuzzy logic has been applied to many SI issues (Takagi and Sugeno 1985, Yan and Langari 1998, Kim et al 2011). A number of studies on Takagi-Sugeno (TS) fuzzy models have been conducted in recent years, and the results provide an effective representation of nonlinear systems with the aid of fuzzy sets, fuzzy rules, and a set of local linear models (Adeli and Samant 2000, Alhanafy 2007, Astrom and Eykhoff 1971, Filev 1991, Gopalakrishnan, et al 2010, Johansen and Babuska 2003, Karim and Adeli 2002). Fuzzy logic theory in the field of large scale infrastructures has been mainly used for nonlinear fuzzy control system design, described by Guo et al (2011). However, determination of the inherent parameters of a fuzzy inference system includes many trial and errors. Therefore, incorporating neural networks allow for automated adjustments of parameters throughout computation.

Neural networks were created to imitate the cognitive mechanism of the human brain. The network is made up of linked nodes, where each node computes an output from its own input. The output of one node is then used as the input for the next node, and a link is created between each node. Neural networks are able to learn throughout the computation by adjusting the parameters to improve performance at each node. This is a useful characteristic of neural networks because it is able to recognize patterns and adjust these parameters in order to better the end result and create a more accurate model. The neural network is useful to determine some of these incomplete measurements to create a full model

of the structure, which can be seen through Hung et al (2003). However, it is challenging to design and analyze the neural networks in a transparent way because it is a black box modeling framework.

An integration of these nonparametric SI models can be made to create a new model, an adaptive neuro-fuzzy inference system (ANFIS). Its application to system identification has been researched by Faravelli et al (1996), Gu and Oyadiji (2008), and Jang et al (1997), but the application of an ANFIS model to the system identification of civil engineering structures is still a relatively new research topic, with work being done by Alhanafy (2007), Faravelli et al (1996), Gopalakrishnan et al (2010), Jalili-Kharaajoo (2004), and Wang (2010). The only structural limitation of this system is that the network configuration must be feedforward to avoid using more complex models. The ANFIS system is able to use a nonlinear system from fuzzy inference systems as well as the adaptive knowledge from neural networks to create a more accurate model. Advantages of the ANFIS system is its ability to create a nonlinear mapping, its use of adjustable parameters, including the membership function (MF) type, the number of MFs, step size, and number of epochs. However, the ANFIS system includes long computation times that can become disadvantageous when dealing in real time.

The incorporation of wavelet transforms to the ANFIS model creates a wavelet-based ANFIS model, or a WANFIS model. The inclusion of the wavelet transform as a means of filtering data greatly reduces computation times for the model, creating a model that outputs comparable results while computing in a fraction of the time. Commonly, Fourier transforms can be used to look at frequency domain responses in dynamics, commonly used for system identification, damage detection, and control systems. A major disadvantage that occurs through the use of Fourier transforms for time-frequency resolutions are the fixed windows, meaning Fourier transforms are allowed to be used for the full scale time window, postulated by Thuillard (2001). However, when using this method in structural dynamics, the time frame is too large to use for real-time damage detection or structural control. Using discrete wavelet transforms in place of Fourier transforms allow for an adjustable window function. It is also used as a filtering method, where it is possible to filter out low or high frequencies, as shown by Thuillard

(2001). Wavelet transforms are a relatively new transformation method that has been developed and studied, as well as its inclusion with other methodologies such as fuzzy logic and neural networks (Adeli, Hojjat, and Kim 2004, Adeli and Karim 2000, Adeli and Samant 2000, Catalao et al 2010, Daubechies 1992, Karim and Adeli 2002, Samant and Adeli 2000, 2001, and Wu and Adeli 2001). The methodology uses multiple levels of discrete wavelet transforms as a means of filtering and de-noising input data. Incorporating discrete wavelet transforms as a means of filtering to the ANFIS system creates the WANFIS system. This methodology has been researched and used in other engineering fields, such as water resource engineering, researched by Guo et al (2011), but is new for the system identification of smart structures, and creates a new model to use for system identification that is computationally efficient. First, the WANFIS identification model is described, followed by simulation results using an earthquake signal excitation.

2.2. Wavelet-based adaptive neuro-fuzzy inference system (WANFIS)

The WANFIS system incorporates a hybrid system to include portions of the wavelet transform, the neural network and fuzzy inference systems. This system is a nonlinear learning model that uses a least-squares method as well as back-propagation methods to train the fuzzy inference system's membership function and its included parameters based on the wavelet-based filtered input and output data sets.

2.2.1. Takagi-Sugeno fuzzy model

Takagi-Sugeno (TS) fuzzy model is the backbone for the proposed WANFIS control system. In 1985, Takagi and Sugeno suggested an effective way for modeling complex nonlinear dynamic systems by introducing linear equations in consequent parts of a fuzzy model, which is called TS fuzzy model (Takagi and Sugeno 1985). It has led to reduction of computational cost because it does not need any

defuzzification procedure. The fuzzy inference system used in the WANFIS model is of the TS fuzzy model form. Typically, it takes the form of

$$R_j\text{: If } u_{FZ}^1 \text{ is } P_{1,j} \text{ and } u_{FZ}^2 \text{ is } P_{2,j} \ldots \text{and } u_{FZ}^i \text{ is } P_{i,j},$$
$$\text{Then } z = f_j\left(u_{FZ}^1, \ldots, u_{FZ}^i\right), \quad j = 1,2, \ldots, N_r, \tag{2-1}$$

where R_j is the j^{th} fuzzy rule, N_r is the number of fuzzy rule, $P_{i,j}$ are fuzzy sets centered at the j^{th} operating point, and u_{FZ}^i are premise variables that can be either input or output values. The equation of the consequent part $z = f\left(u_{FZ}^1, \ldots, u_{FZ}^i\right)$ can be any linear equation. Note that the Eq. (2-1) represents the j^{th} local linear subsystem of a nonlinear system, i.e., a linear system model that is operated in only a limited region. All of the local subsystems are integrated by blending operating regions of each local subsystem using the fuzzy interpolation method as a global nonlinear system

$$y = \frac{\sum_{j=1}^{N_r} W_j\left(u_{FZ}^i\right)\left[f_j\left(u_{FZ}^1, \ldots, u_{FZ}^i\right)\right]}{\sum_{j=1}^{N_r} W_j\left(u_{FZ}^i\right)}, \tag{2-2}$$

where $W_j\left(u_{FZ}^i\right) = \prod_{i=1}^{n} \mu_{P_{i,j}}\left(u_{FZ}^i\right)$ and $\mu_{P_{i,j}}\left(u_{FZ}^i\right)$ is the grade of membership of u_{FZ}^i in$P_{i,j}$. These parameters are optimized by the back propagation neural network. A typical architecture of fuzzy rules are shown in figure 2-1, which shows four membership functions and sixteen rules, whereas the model in this paper uses only two membership functions and four rules.

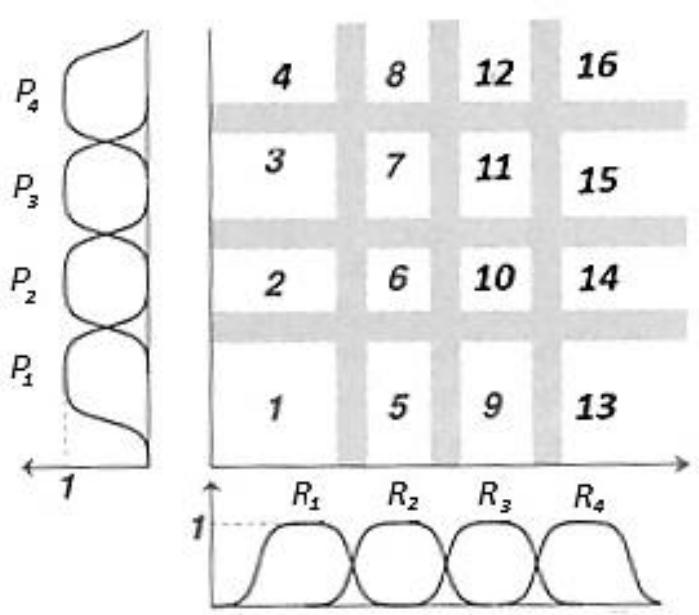

Figure 2-1. Typical fuzzy rules layout [20]

The main challenge in using a fuzzy model is the optimization of the parameters of the model. Therefore, incorporating neural networks to create an adaptive neuro-fuzzy inference system allows for these parameters to be optimized during computation, which is explained below.

2.2.2. ANFIS architecture

The architecture of an ANFIS model typically looks similar to figure 1-2.

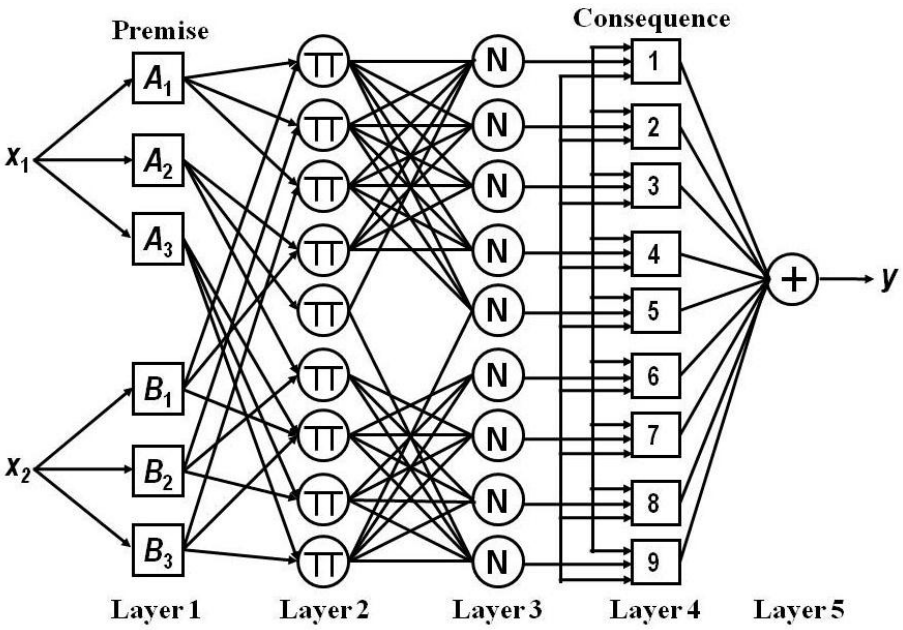

Figure 2-2. ANFIS architecture

This figure represents a two input, one output, and three MFs system. Each layer has particular tasks to complete before the data moves to the next layer. In layer 1, the function of the node is represented by

$$F_{FZ}^{1,j} = \mu_{P_{i,j}}\left(u_{FZ}^{i}\right). \tag{2-3}$$

For a Gaussian MF used in this simulation,

$$\mu_{P_{i,j}}(u_{FZ}^{i}) = exp\left[-\frac{(u-a_1)^2}{2a_2^2}\right], \quad (2\text{-}4)$$

where a_1 and a_2 are adjustable parameters of the Gaussian function. This MF is applied to each input in layer 1. Layer 2 then outputs the product of all inputs into layer 2, known as the firing strength

$$F_{FZ}^{2,j} = \mu_{P_{i,j}}(u_{FZ}^{1}) \times \mu_{P_{i,j}}(u_{FZ}^{2}) \dots \mu_{P_{i,j}}(u_{FZ}^{i}). \quad (2\text{-}5)$$

Layer 3 takes a ratio of these layer 2 firing strengths in order to normalize the layer 2 outputs, such that

$$F_{FZ}^{3,j} = F_{FZ}^{2,j} / \sum_j \prod_{i=1}^{n} \mu_{P_{i,j}}(u_{FZ}^{i}). \quad (2\text{-}6)$$

Layer 4 then applies a node function to the normalized firing strengths

$$F_{FZ}^{4,j} = F_{FZ}^{3,j} * f_j = F_{FZ}^{3,j}\left[f_j(u_{FZ}^{1}, \dots, u_{FZ}^{i})\right], \quad (2\text{-}7)$$

where a_3, a_4, a_5 are function parameters for the consequent. The last layer summates the layer inputs

$$F_{FZ}^{5} = \frac{\sum_j \prod_{i=1}^{n} \mu_{P_{i,j}}(u_{FZ}^{i})\left[f_j(u_{FZ}^{1}, \ldots, u_{FZ}^{i})\right]}{\sum_j \prod_{i=1}^{n} \mu_{P_{i,j}}(u_{FZ}^{i})}. \quad (2\text{-}8)$$

The output of this system is then used in a hybrid learning algorithm to create a linear combination of the consequent parameters, a_3, a_4, a_5. The key parameters for this simulation include the number of iterations, or epochs, the number of MFs and the type of MF, as well as the step size of the function. Types of MFs can vary from a generalized bell function, Gaussian functions, sigmoidal functions, trapezoidal function, as well as other forms. Each change of variables will yield different output results, shown by Filev (1991) and Kim et al. (2011). The fuzzy inference system sets up rules based on the number of MFs used in simulation. For a four MF system, the following fuzzy rules are set up and shown in figure 2-1, where F_{FZ}^{5} corresponds to *y*. Each number represents one of the sixteen fuzzy regions that are created through the use of four MF s in the ANFIS model. The fuzzy region is defined by the premise, and the output is generated through the consequent.

Although the ANFIS is very effective in modeling complex nonlinear systems, it requires much computational loads. Such a problem can be addressed through the integration of wavelet transform-based multi-resolution analysis framework.

2.2.3. Wavelet transform

Wavelet analysis began during the 1980s by Morlet, who discovered the use of wavelet analysis in signal processing, detailed by Thuillard (2001). It was created by modifying previous mathematical concepts such as Fourier analyses, where the time window is fixed to include the entirety of the signal. Wavelet theory began by bypassing this drawback of the Fourier analysis so that wavelet analysis used a variable time-window, allowing for scientists and engineers to look at a specific time frame of the signal for signal analysis. Mathematicians working with filter theory were able to use this concept of wavelet analysis and

apply it to their field, and reconstruction filters were developed. This meant that signals were able to be divided into sampled signals and then reconstructed into a signal that is equivalent to the original signal. Mallat (1989) created a fast wavelet decomposition algorithm to compute the wavelet coefficients using the wavelet filters, with one algorithm for decomposition of the signal and another algorithm for the reconstruction to the equivalent signal. Being able to reconstruct a signal using these algorithms provides the ability for data compression and noise reduction, shown by Thuillard (2001).

Fourier transforms and its modifications, such as short-time Fourier transforms and fast Fourier transforms, use a fixed time-frequency resolution, causing an issue in many engineering applications, mainly an inability to see low or high frequency portions of the window when viewing the entire window. A continuous wavelet transform was developed from the Fourier analysis, such that:

$$W_\Psi f(a,b) = 1/\sqrt{a} \int_{-\infty}^{\infty} f(x) * \Psi^* \left(\frac{x-b}{a}\right) dx, \quad \text{(2-9)}$$

where a is a scaling factor, b is the width of the window in the time domain, and Ψ is the wavelet function. From the continuous wavelet transform, the discrete wavelet transform can be derived, and is given as:

$$u_{FZ}^i = 2^{(s/2)} \sum_n x_i(n)\ \emptyset(2^s t - l), \quad \text{(2-10)}$$

and the original signal, $x(n)$, can be recalculated from the wavelet function using

$$x_i(n) = \sum_l \sum_s u_{FZ}^i \Psi_{l,s}(n), \quad \text{(2-11)}$$

where l is the location index, s is the scale index, and $\emptyset$ is the mother function. Using discrete wavelet transforms allows for the isolation of high frequency components from the signal at the time they occur. This results in a signal of low frequency components with continuous magnitudes. In order to look at both high and low frequency portions of the signal, multi-resolution analysis should be investigated.

Multi-resolution analysis (MRA) was developed to decompose a function into slowly-varying and rapidly-varying segment signals, allowing for the divided function segments to be studied separately. This allows for a representation of the function at a single level of approximation by discretizing the function using the step size, and therefore significantly reducing the total number of data points needed to accurately represent the signal, which is also known as filtering the data signal. In essence, MRA decomposes a signal into multiple levels of resolution, or most commonly, into high frequency and low frequency resolutions. Studying the low frequency components provides the main features of the signal, while features of the high frequency resolution component can be useful in fields such as damage detection (Thuillard 2001). The scaling function for the formulation of the wavelet transform in order to mathematically represent the MRA is

$$\emptyset_{l,s} := 2^{s/2}\emptyset(2^s t - l), \tag{2-12}$$

and the wavelet is given by

$$\Psi_{l,s} := 2^{s/2}\Psi(2^s t - l), \tag{2-13}$$

where Ψ is the scaling function. The scaling function is used to stretch or compress the function in the selected time domain. Any function $x_s(t)$ and $y_s(t)$ can be represented as the linear combination of $\emptyset_{l,s}(t)$ and $\Psi_{l,s}(t)$, respectively. The functions $x_{s-1}(t) \in A_{s-1}$ and $y_{s-1}(t) \in W_{s-1}$ are developed from $x_s \in A_s$, where W_s is called the wavelet subspace and is complimentary to A_s in A_{s+1} such that the intersection of A_s and W_s does not exist and the summation of A_s and W_s creates A_{s+1}. A typical graphical representation of this MRA is shown in figure 2-3.

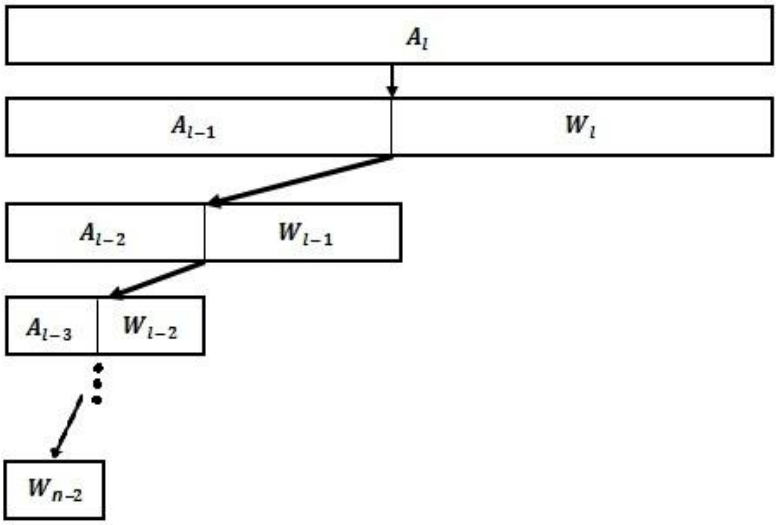

Figure 2-3. Wavelet transform-based multi-resolution analysis framework

2.2.4. Wavelet-based ANFIS system identification

The inclusion of discrete wavelet transforms allow for an effective method to rid responses of extraneous data, or noise. This methodology uses Daubechie filters for low frequency decomposition in order to de-noise response data that is then used as inputs to the ANFIS model. As mentioned earlier, the use of wavelet transforms allows for a fixed time-frequency resolution, meaning the window function is chosen, and then the resolution is fixed through processing. Representation of the function with several discretization steps allows for a reduction in the number of data points required for accurate representation of the system. This model proposes the use of two levels of discrete wavelet transforms as a means of filtering as well as applying the ANFIS methodology to train to the control force of an optimal controller. The architecture of this proposed WANFIS system is depicted in figure 2-4.

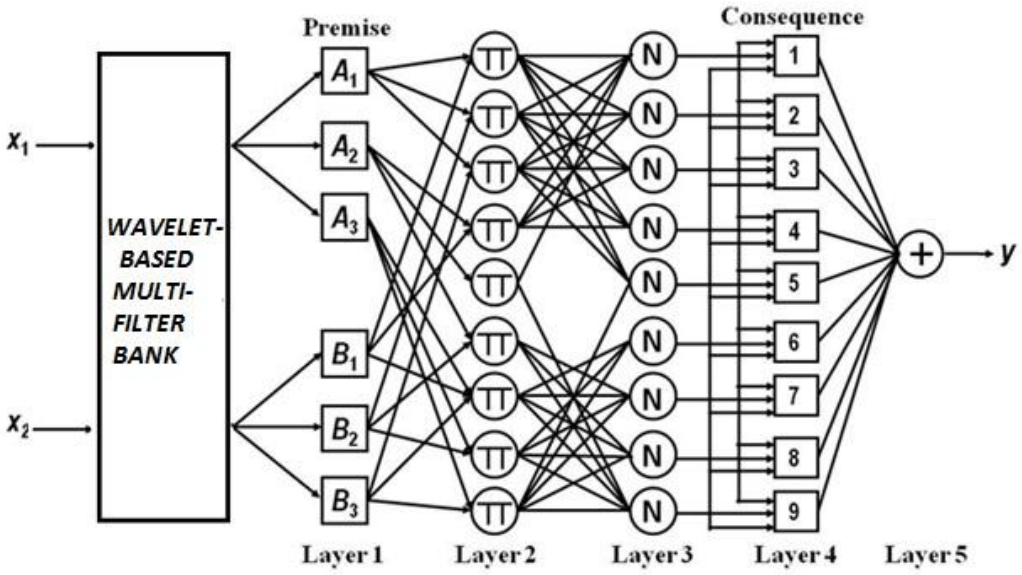

Figure 2-4. WANFIS architecture

Next, simulations were performed to train the WANFIS model to the nonlinear response of a three-story building equipped with a magnetorheological damper subjected to an artificial earthquake. Then, the model was validated using known earthquake signals, including the El-Centro, Kobe, Hachinohe, and Northridge earthquakes.

2.3. Example

To demonstrate the effectiveness of the wavelet-based adaptive neuro-fuzzy inference system (WANFIS) approach, a three-story building structure equipped with a magnetorheological (MR) damper is investigated.

2.3.1 Magnetorheological (MR) Damper

In recent years, smart structures have emerged from many engineering fields because the performance of structural systems can be improved without either significantly increasing the structure mass or requiring

high cost of control power. They may be called intelligent structures, adaptive structures, active structures, and the related technologies adaptronics, structronics, etc. The reason to use these terminologies is that a smart structure is an integration of actuators, sensors, control units, and signal processing units with a structural system. The materials that are commonly used to implement the smart structure: piezoelectrics, shape memory alloys, electrostrictive, magnetostrictive materials, polymer gels, magnetorheological fluid, etc., researched in detail by Hurlesbaus and Gaul (2006).

Semiactive control systems have been applied to large structures because the semiactive control strategies combine favorable features of both active and passive control systems. Semiactive control devices include variable-orifice dampers, variable-stiffness devices, variable-friction dampers, controllable-fluid dampers, shape memory alloy actuators, piezoelectrics, etc., as described by Hurlesbaus and Gaul (2006). In particular, one of the controllable-fluid dampers, magnetorheological (MR) damper has attracted attention in recent years because it has many attractive characteristics.

In general, a MR damper consists of a hydraulic cylinder, magnetic coils, and MR fluids that consist of micron-sized magnetically polarizable particles floating within oil-type fluids as shown in figure 2-5.

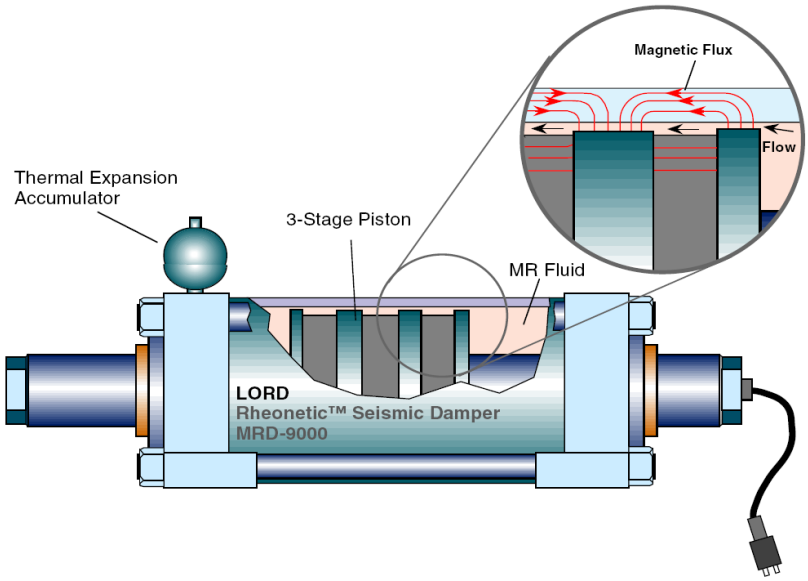

Figure 2-5. Schematic of the prototype 20-ton large-scale MR damper (Kim et al, 2009)

The MR damper is operated as a passive damper; however, when a magnetic field is applied to the MR fluids, the MR fluids are changed into a semi-solid state in a few milliseconds. This is one of the most unique aspects of the MR damper compared to active systems: the active control system malfunction might occur if some control feedback components, e.g., wires and sensors, are broken for some reasons during severe earthquake event; while a semiactive system is still operated as at least a passive damping system even when the control feedback components are not functioning properly. Its characteristics are summarized by Kim et al. (2009).

To fully use the best features of the MR damper, a mathematical model that portrays the nonlinear behavior of the MR damper has to be developed first. However, this is challenging because the MR damper is a highly nonlinear hysteretic device. As shown in figure 2-6, determined by Spencer et al. (1997), the MR damper force $f_{MR}(t)$ predicted by the modified Bouc-Wen model is governed by the following differential equations

$$f_{MR} = c_a \dot{u}_b + k_a(u_a - u_{a0}), \tag{2-14}$$

$$\dot{z}_{BW} = -\gamma|\dot{u}_a - \dot{u}_b|z_{BW}|z_{BW}|^{n-1} - \beta(\dot{u}_a - \dot{u}_b)|z_{BW}|^n + A(\dot{u}_a - \dot{u}_b), \tag{2-15}$$

$$\dot{u}_b = \frac{1}{(c_a + c_b)}\{\alpha z_{BW} + c_b \dot{u}_a + k_b(u_a + u_b),\} \tag{2-16}$$

$$\alpha = \alpha_a + \alpha_b u, \tag{2-17}$$

$$c_a = c_{a1} + c_{a2} u, \tag{2-18}$$

$$c_b = c_{b1} + c_{b2} u, \tag{2-19}$$

$$\dot{u} = -\eta(u - v) \tag{2-20}$$

where z_{BW} and α called evolutionary variables, describe the hysteretic behavior of the MR damper; c_b is the viscous damping parameter at high velocities; c_a is the viscous damping parameter for the force roll-off at low velocities; α_a, α_b, c_{b1}, c_{b2}, c_{a1}, and c_{a2} are parameters that account for the dependence of the MR damper force on the voltage applied to the current driver; k_b controls the stiffness at large velocities; k_a represents the accumulator stiffness; u_{a_0} is the initial displacement of the spring stiffness k_a; γ, β and A are adjustable shape parameters of the hysteresis loops, i.e., the linearity in the unloading and the transition between pre-yielding and post-yielding regions; v and u are input and output voltages of a first-order filter, respectively; and η is the time constant of the first-order filter.

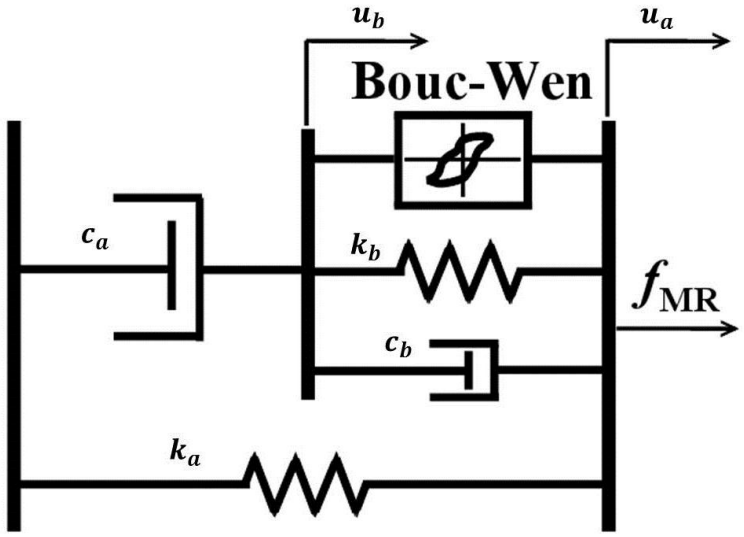

Figure 2-6. Modified Bouc-Wen model of the MR damper

Note that nonlinear phenomena occur when the highly nonlinear MR dampers are applied to structural systems for effective energy dissipation. Such an integrated structure-MR damper system behaves nonlinearly although the structure itself is usually assumed to remain linear. Therefore, the development of a mathematical model that portrays nonlinear behavior of the structure-MR damper system would play a key role in semiactive control system design. The MR damper parameters are provided in Table 2-1.

Table 2-1. Parameters of MR damper (Kim et all, 2009)

Parameter	Value	Parameter	Value
c_{b1}	21.0 N-s-cm^{-1}	α_a	140 Ncm^{-1}
c_{b2}	3.50 N-s-cm^{-1}V^{-1}	α_b	695 Ncm^{-1}V^{-1}
k_b	46.9 Ncm^{-1}	Γ	363 cm^{-2}
c_{a1}	283 Nscm^{-1}	B	363 cm^{-2}
c_{a2}	2.95 Nscm^{-1}V^{-1}	A	301
k_a	5.00 Ncm^{-1}	N	2
u_{a_0}	14.3 cm	H	190 s^{-1}

2.3.2 Integrated structure-MR damper system

A typical example of a building structure employing an MR damper is depicted in Figure 2-7.

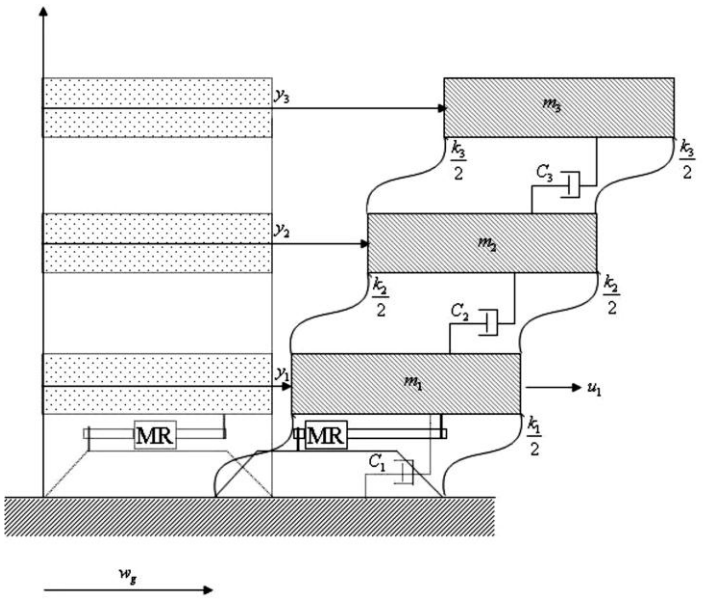

Figure 2-7. A 3-story building employing an MR Damper

Note that the MR damper can be installed at arbitrary locations within the building structure. Although the locations that the MR dampers are installed within the building can be optimized via optimization procedures, this issue is beyond the scope of this paper. The associated equation of motion is given by

$$\mathbf{M}\ddot{x} + \mathbf{C}\dot{x} + \mathbf{K}x = \mathbf{\Gamma} \boldsymbol{f}_{\boldsymbol{MR}}(t, x_i, \dot{x}_i, v_i) - \mathbf{M}\mathbf{\Lambda}\ddot{w}_g, \tag{2-21}$$

where: $\ddot{w}_g$ denotes the ground acceleration, $\mathbf{M}$ the mass matrix, $\mathbf{K}$ the stiffness matrix, $\mathbf{C}$ the damping matrix, and the vector x the displacement relative to the ground, $\dot{x}$ the velocity, $\ddot{x}$ the acceleration; x_i and $\dot{x}_i$ are the displacement and the velocity at the i^{th} floor level relative to the ground, respectively, v_i is the voltage level to be applied, and $\mathbf{\Gamma}$ and $\mathbf{\Lambda}$ are location vectors of control forces and disturbance signal, respectively. The second order differential equation can be converted into a state space model

$$\dot{\boldsymbol{z}} = \mathbf{A}\boldsymbol{z} + \mathbf{B}\boldsymbol{f}_{\mathbf{MR}}(t, x_i, \dot{x}_i, v_i) - \mathbf{E}\ddot{w}_g,$$
$$\boldsymbol{y} = \mathbf{C}\boldsymbol{z} + \mathbf{D}\boldsymbol{f}_{\mathbf{MR}}(t, x_i, \dot{x}_i, v_i) + \boldsymbol{n}, \tag{2-22}$$

where

$$\mathbf{A} = \begin{bmatrix} 0 & \mathbf{I} \\ -\mathbf{M}^{-1}\mathbf{K} & -\mathbf{M}^{-1}\mathbf{C} \end{bmatrix} \tag{2-23}$$

$$\mathbf{B} = \begin{bmatrix} \mathbf{0} \\ \mathbf{M}^{-1}\mathbf{F} \end{bmatrix} \tag{2-24}$$

$$\mathbf{C} = \begin{bmatrix} \mathbf{I} & 0 \\ 0 & \mathbf{I} \\ -\mathbf{M}^{-1}\mathbf{K} & -\mathbf{M}^{-1}\mathbf{C} \end{bmatrix} \tag{2-25}$$

$$\mathbf{D} = \begin{bmatrix} 0 \\ 0 \\ \mathbf{M}^{-1}\mathbf{F} \end{bmatrix} \tag{2-26}$$

$$\mathbf{E} = \begin{bmatrix} 0 \\ \mathbf{F} \end{bmatrix} \tag{2-27}$$

where **F** is the location matrix that Chevron braces are located within the building structure, $\boldsymbol{n}$ is the noise vector, and x_i and $\dot{x}_i$ are the displacement and the velocity at the i^{th} floor level of the three-story building structure, respectively. Properties of the three-story building structure are adopted from Yang et al. (2002).

2.3.3 Simulation

To show the effectiveness of the WANFIS model for SI, a set of input-output data is generated for training from a seismically excited building structure equipped with an MR damper. An artificial

earthquake excitation signal and MR damper forces are applied to the smart structure to generate output data: displacement and acceleration. The parameters that affect the system are the MF type, number of MFs, step size, number of epochs, and the filter used. This simulation uses a two-level wavelet filter to rid the signal of its noise.

The architecture of the WANFIS model is determined via trial-and-error strategies: the number of MFs is chosen to be 2; Gaussian MFs are used as the design variables, with a number of epochs of 200 and a step size of 0.001, for the artificial earthquake signal. Figure 2-8 and figure 2-9 are shown for a graphical representation of the input forces from the artificial earthquake signal and the MR damper, respectively.

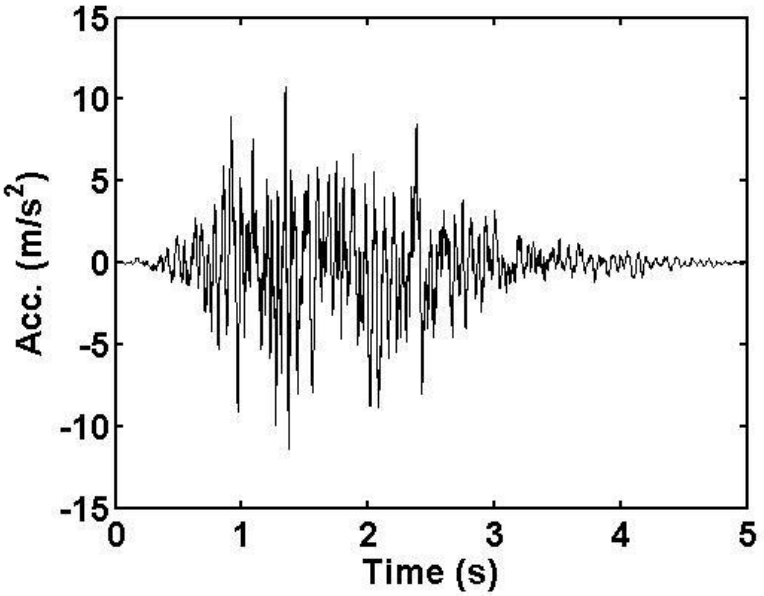

Figure 2-8. Artificial earthquake signal

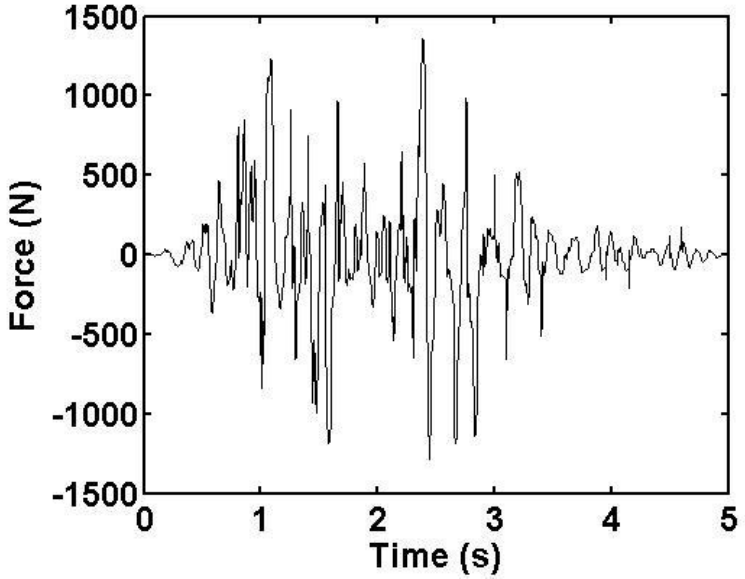

Figure 2-9. MR Damper force

Figures 2-10, 2-11, 2-12, and 2-13 show the earthquake signals for the four validation earthquakes.

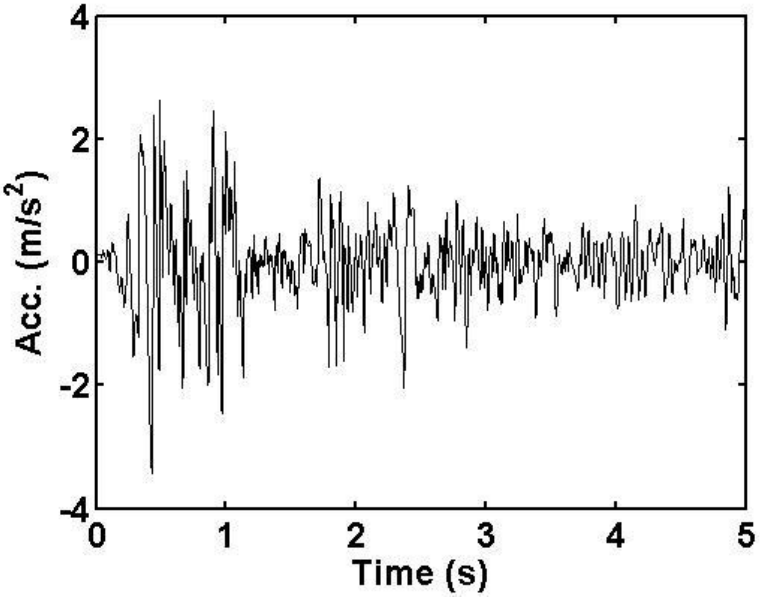

Figure 2-10. 1940 El-Centro earthquake signal

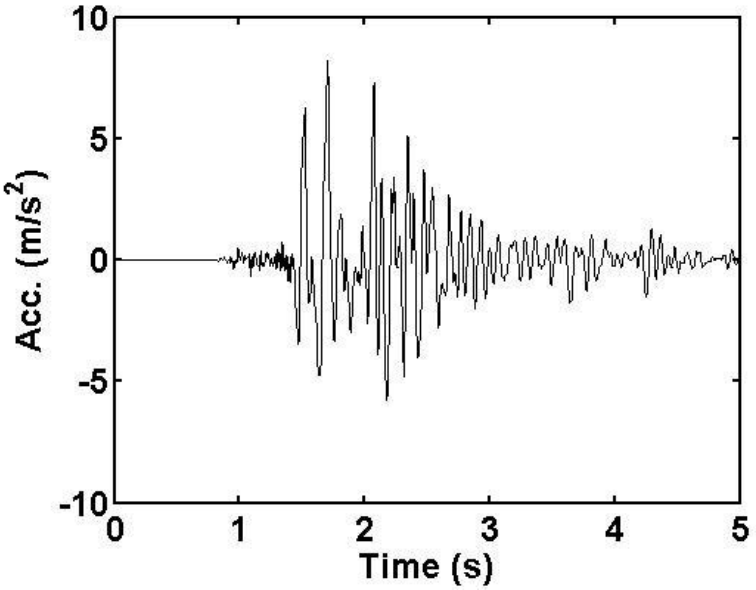

Figure 2-11. Kobe earthquake signal

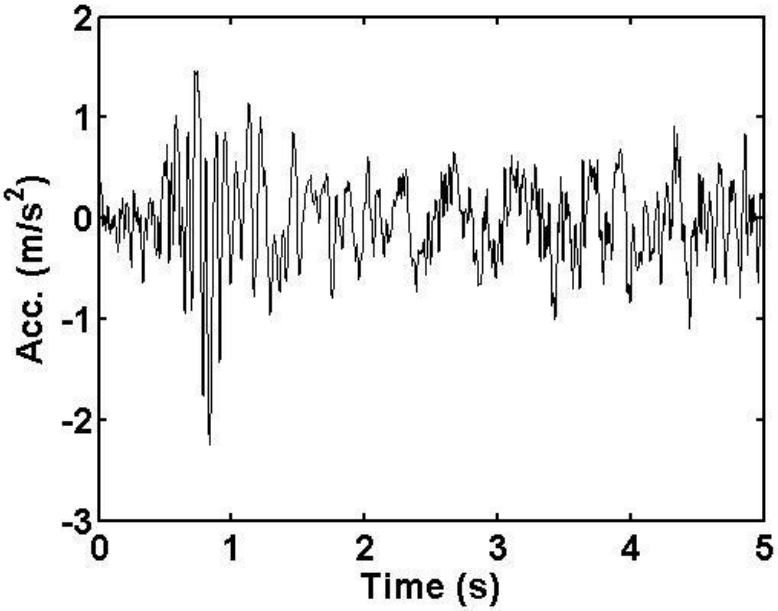

Figure 2-12. Hachinohe earthquake signal

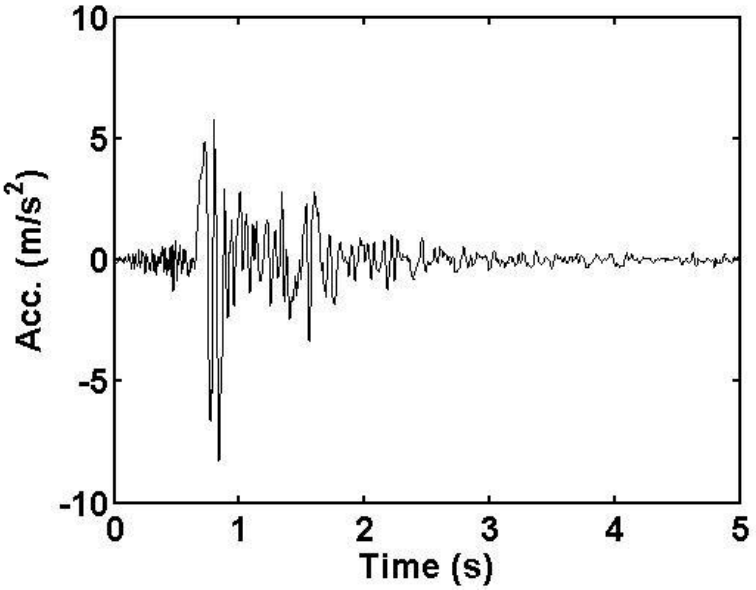

Figure 2-13. Northridge earthquake signal

Although the architecture of the WANFIS model can be optimized through an optimization procedure, it is beyond the scope of the present paper. The performance of the identified model can be improved by increasing either the number of MFs or the step size, resulting in greater accuracies between the training data and the dynamic signal. However, these increased parameters (i.e., overtraining) may not be an efficient approach for validating the developed model using other data sets. Furthermore, it is not guaranteed that the larger number of MFs, the better performance of the WANFIS system.

Figure 2-14 depicts the comparison of the dynamic response of the original simulation model with that of the identified WANFIS model using an artificial earthquake signal. Note that the original simulation model means an analytic model of the building equipped with an MR damper.

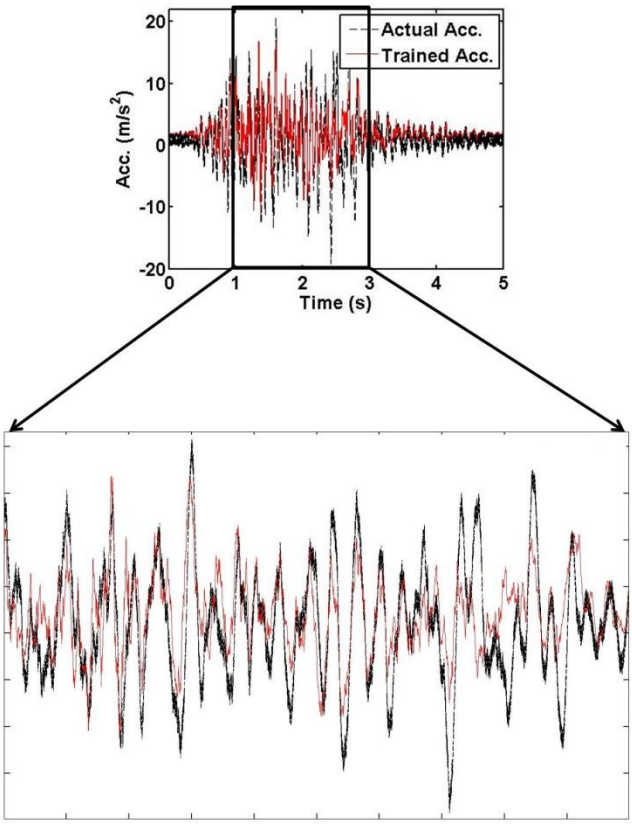

Figure 2-14. Comparison of dynamic responses of simulation data and training data (Artificial earthquake)

As seen, overall good agreements between the original values and the identified WANFIS models are found in the dynamic responses. As discussed previously, the performance of the WANFIS model can be improved by increasing input parameters, which can also significantly increase computation time. Figures 2-15. 2-16, 2-17, and 2-18 show comparisons of the actual accelerations of the third story and the response obtained from validation for each of the four validating earthquakes, El-Centro, Kobe, Hachinohe, and Northridge.

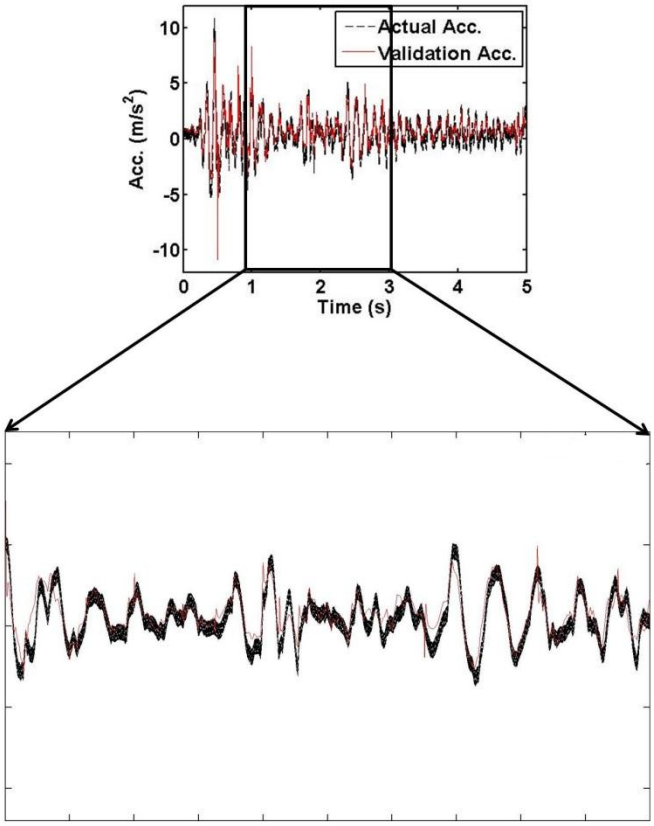

Figure 2-15. Comparison of dynamic responses of simulation data and validation data (El-Centro earthquake)

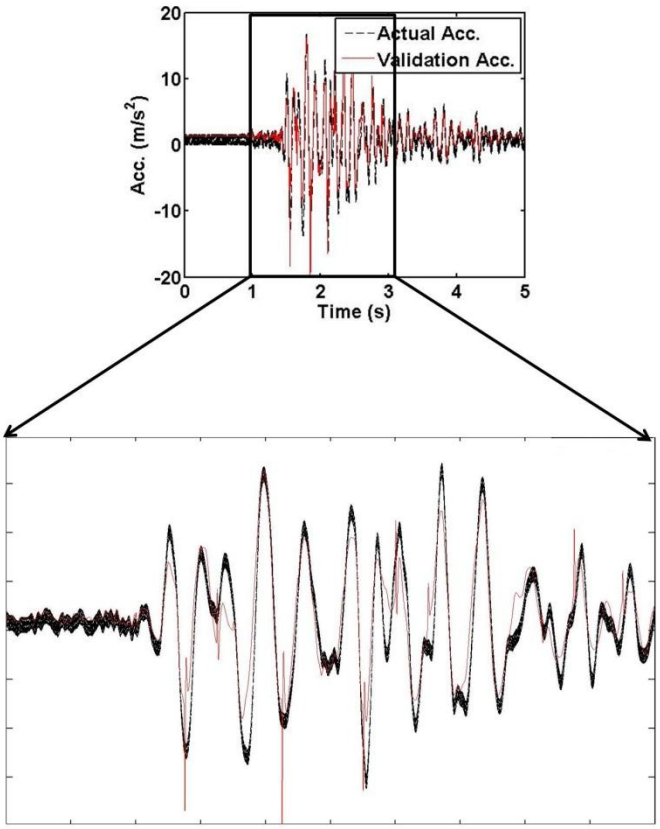

Figure 2-16. Comparison of dynamic responses of simulation data and validation data (Kobe earthquake)

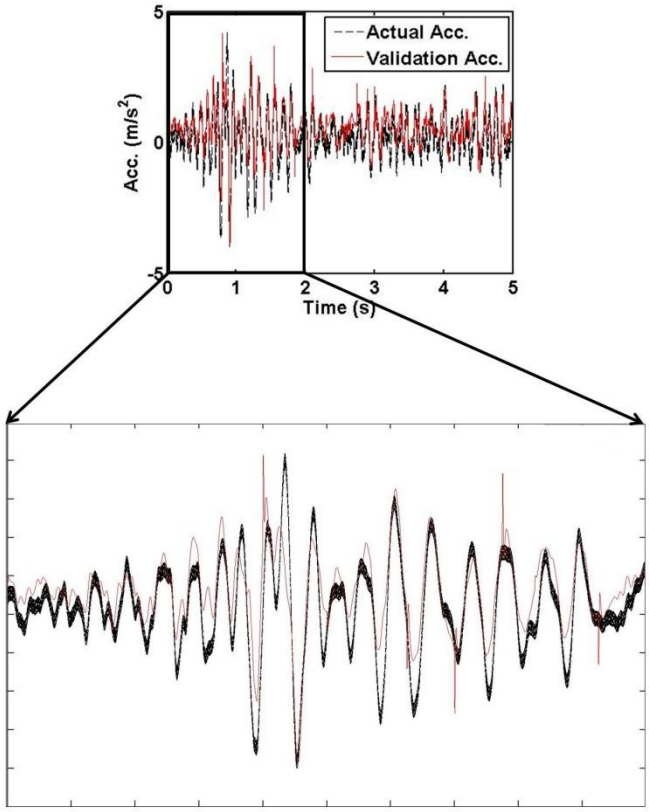

Figure 2-17. Comparison of dynamic responses of simulation data and validation data (Hachinohe earthquake)

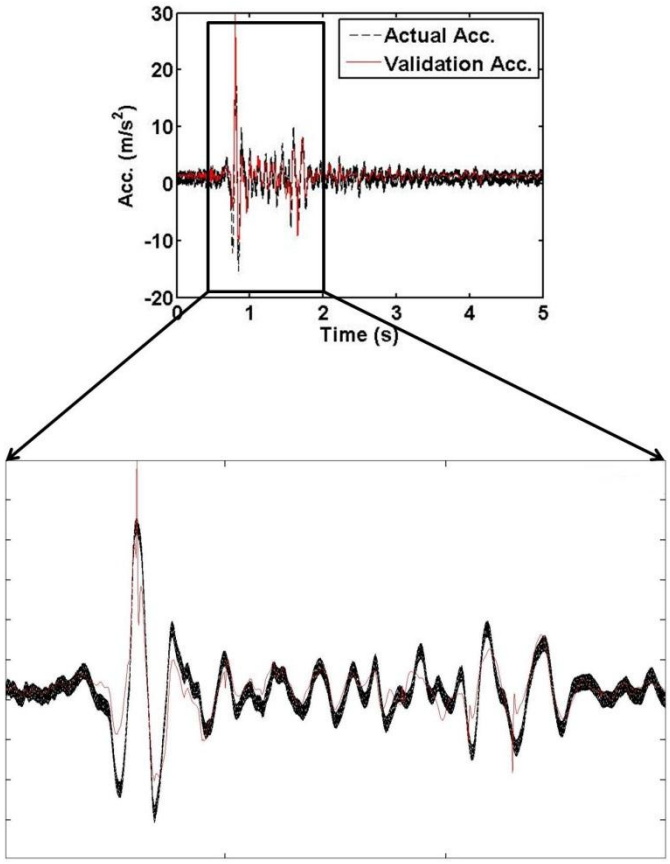

Figure 2-18. Comparison of dynamic responses of simulation data and validation data (Northridge earthquake)

It is shown from the figures that the validation responses correlate well with the actual accelerations, meaning that the proposed WANFIS model is effective in modeling the nonlinear dynamic response of a structure employing an MR damper.

In order to quantify the error and relationship between the trained model and the actual response of the structure, a root mean square error (RMSE) is obtained. It can be formulated into an equation as

$$J_1 = E(\tilde{y} - \hat{y})^2 \tag{2-28}$$

where $\hat{y}$ is the estimation, $\tilde{y}$ is the actual structural response data, and N is the number of data points. Another index to use can be formulated as

$$J_2 = \left[1 - \frac{\tilde{y} - \hat{y}}{\tilde{y} - \bar{y}}\right] \times 100 \tag{2-29}$$

where $\bar{y}$ is the mean value of the actual structural response data, $\tilde{y}$. Note that if the WANFIS model produces the same responses as the simulation model, the fitting rate J_2 is 100. The training results of the artificial earthquake and responses are provided in Table 2-2.

Table 2-2. Training errors and times

System	Training Time (sec)	Max RMSE (cm/s^2)	Min RMSE (cm/s^2)	Mean RMSE (cm/s^2)	$\left[1 - \frac{\lvert\tilde{y} - \hat{y}\rvert}{\lvert\tilde{y} - \bar{y}\rvert}\right] \times 100$
ANFIS	4815.120	1824.5	0.7203	1032.2	83.137
WANFIS1	1392.174	1823.2	1.2704	972.2	81.193
WANFIS2	445.812	1839.9	2.8403	1028.4	86.125

The WANFIS2 model is optimized using the artificial earthquake signal, with a total training time of 7.4302 minutes, or 445.812 seconds. It is also found that the fitting rate J_2 of the WANFIS model is better than the ANFIS model. The validation errors are provided in Table 2-3 for each earthquake.

Table 2-3. Validation of the trained model

WANFIS 2 System	El-Centro	Kobe	Northridge	Hachinohe
Max. RMSE (cm/s^2)	9.2476	16.4820	26.5756	3.8991
Min. RMSE (cm/s^2)	0.0026	0.0068	0.0084	0.0034
Mean RMSE (cm/s^2)	9.7961	10.1886	5.5438	0.8987
$\left[1 - \frac{\lvert\tilde{y} - \hat{y}\rvert}{\lvert\tilde{y} - \bar{y}\rvert}\right] \times 100$	82.160	69.199	57.667	68.652

Although for the training data, the ANFIS model resulted in a slightly better RMSE value, the WANFIS2 model is preferred due to the more favorable computation times, quantified as roughly 90% less computation time. For validation purposes, the WANFIS2 model resulted in a lower RMSE value for each of the four validation earthquakes than the ANFIS model.

2.4. Conclusion

In this paper, a novel wavelet-based adaptive neuro-fuzzy inference system (WANFIS) is proposed for nonlinear system identification of seismically-excited smart building structures that are equipped with magnetorheological (MR) dampers. The WANFIS is an integrated model of Takagi-

Sugeno fuzzy model, wavelet transforms, and artificial neural networks. Using a WANFIS system combines the positive attributes of the three described methodologies to create a system that is believed to yield more efficient results for system identification of smart structures and shorter training times. To train the input-output mapping function of the WANFIS model, an artificial earthquake signal and an MR damper force signal are used as a disturbance input signal and a control input, respectively, while acceleration response is used as output data. This approach can be applied to an integrated model of a primary building structure and nonlinear MR devices without decoupling the identification procedure of the highly nonlinear MR damper from that of the primary building structure. It is demonstrated from the simulation that the proposed WANFIS model is effective in identifying the nonlinear behavior of the seismically excited building-MR damper system while shortening the training time typical of an ANFIS model.

The nonlinear system identification framework for identifying nonlinear behavior of the smart building-MR damper systems addressed in this paper has been demonstrated numerically. Further research is recommended to verify the effectiveness of the proposed methodologies experimentally.

3. Wavelet-Neuro-Fuzzy Control of Hybrid Building-ATMD System under Seismic Excitations[2]

3.1. Introduction

An important aspect of structural dynamics is the mitigation of detrimental structural responses when a structure is subjected to a forced excitation. During a dynamic loading event, such as an earthquake or strong winds, structures may experience large displacements, velocities, and accelerations that can become detrimental to the integrity of the structure. Loss of structural integrity in a building or a bridge, for example, may be caused by excessive cracks and strength degradation and could result in severe damage or collapse to local elements or the structure as a whole. Because of the severe ramifications that may result from earthquake acting on a structure, control devices can be mounted in a building in order to reduce the structural response and create a system that will function adequately and safely following a seismic event. These devices induce a force into the structure in order to offset the internal forces and accelerations that the structure experiences during an earthquake.

Control systems are typically divided into three categories: passive control systems, active control systems, and hybrid control systems. Passive control systems include devices that are installed during the construction of the structure and may not be modified throughout the structure's lifetime. They are always on-line, meaning that the force exerted from the passive control device is always being used as a dissipative energy input into the structural system without any use of electrical power. Examples of passive control devices include base isolation

[2] This paper has been accepted into the *Journal of Vibration and Control*.

systems and viscous fluid dampers, which are common in structures equipped with control systems since they are easy to implement and cost-effective. Active control systems typically include actuators to input a force into the system in real-time, meaning the force is exerted during a seismic event. The actuator force placed on the structure is time-varying, meaning that the magnitude and/or frequencies of the force changes in time, depending on the magnitude of the external acceleration the structure is subjected to. Therefore, if there is a malfunction with the device, the actuator will output an inappropriate force or no force at all, leaving the building exposed to large, uncontrolled responses, damage, or collapse.

Due to the drawbacks of these two systems, hybrid control systems can be used to incorporate the positive attributes of both passive and active control systems. These systems have passive control devices to constantly keep the structure on-line and provide a means of control if an issue arises with the active and/or semiactive control device, which uses a tuned mass damper with an actuator. This system is versatile and adaptable, able to adjust in real-time due to a control algorithm involved in the active control system. Such hybrid control systems have been studied by many investigators (Housner et al. 1994; Kareem et al. 1999; Nishitani and Inoue 2001; Yang and Dyke 2003; Casciati 2003; Faravelli and Spencer et al. 2003; Kim and Roschke 2006; Kim and Roschke 2007; Ozbulut et al. 2011). In this study, the proposed hybrid control system consists of a tuned mass damper, viscous liquid dampers, and an actuator. The system involves a passive viscous liquid damper located on each floor, along with an active tuned mass damper (ATMD) placed on the top floor of the building. The ATMD includes an actuator to create the active control portion of the hybrid control system, and the system uses a Wavelet-based Adaptive Neuro-Fuzzy Inference System (WANFIS) control algorithm. This algorithm combines the effects of fuzzy logic theory and neural networks to create an adaptive

neuro-fuzzy inference system (ANFIS) system, and then is combined with wavelet theory to filter the response data. This system is detailed further below.

A fuzzy inference system uses fuzzy set theory to create a set of rules with which the system must follow, and is commonly used as a nonparametric identification method. It is effective in showing the complexities that arise from nonlinearities and dynamic system uncertainties (Kim et al., 2009a; Langari, 1999). Since Zadeh's paper (Zadeh, 1965), fuzzy logic has been applied to many system identification (SI) issues (Takagi and Sugeno, 1985; Zadeh, 1965; Kim and Langari, 2007; Kim et al., 2009b; Kim et al., 2011). A number of studies on Takagi-Sugeno (TS) fuzzy models have been conducted in recent years, and the results provide an effective representation of nonlinear systems with the aid of fuzzy sets, fuzzy rules, and a set of local linear models (Chen et al., 2007; Du and Zhang, 2008; Faravelli and Yao, 1996; Johansen, 1994; Johansen and Babuška, 2003; Takagi and Sugeno, 1985; Yager and Filev, 1993; Yan and Zhou, 2006; Kim et al. 2010a-b). However, one challenge of the fuzzy inference system is optimizing the parameters of the fuzzy model. Therefore, the use of neural networks can be helpful.

Neural networks were created to imitate the cognitive mechanism of the human brain. The network is made up of linked nodes, where each node computes an output from its own input. The output of one node is then used as the input for the next node, and a link is created between each node. Neural networks are able to learn throughout the computation by adjusting the parameters to improve performance at each node. This is a useful characteristic of neural networks because it is able to recognize patterns and adjust these parameters in order to improve the end result and create a more accurate model. The neural network is useful to determine some of these incomplete measurements to create a full model of the structure (Hung et al., 2003). A

main challenge with using neural networks is the amount of computation time that the model can take. Wavelet transforms can be used as a means of filtering data and reducing the computation time, and is explained further below.

The incorporation of wavelet transforms to the ANFIS model creates a wavelet-based ANFIS model, or a WANFIS model. Fourier transform can be used to look at frequency domain responses in dynamics, commonly used for system identification, damage detection, and control systems. A major disadvantage that occurs through the use of Fourier transforms for time-frequency resolutions are the fixed windows, meaning Fourier transforms are allowed to be used for the full scale time window. However, when using this method in structural dynamics, real-time time windows are looked at, and therefore the time frame is too large to use for damage detection or structural control. Using discrete wavelet transforms in place of Fourier transforms allow for an adjustable window function. It is also used as a filtering method, where it is possible to filter out low or high frequencies. In this study, the methodology uses two levels of discrete wavelet transforms as a means of filtering and de-noising input data.

This proposed WANFIS system as a control algorithm is new to the field of control systems for hazard mitigation of large infrastructures. Previously, fuzzy logic controllers have been used and researched (Ahlawat and Ramaswamy, 2002). From this, ANFIS controllers were used (Gu and Oyadiji, 2008; Hashim et al., 2004), but using a WANFIS controller in place of ANFIS controllers provide much shorter computation times. The proposed WANFIS control algorithm has many contributions, including dramatically reducing computation times from a standard ANFIS system, require less feedback information compared to full state feedback controllers and, as a result, less sensors in the structure, and better structural performance in

comparison to other commonly used control systems. First, the WANFIS model is described, followed by simulation results using a variety of earthquake signal excitations.

3.2. Wavelet-based adaptive neuro-fuzzy inference system (WANFIS)

The WANFIS system incorporates a hybrid system to include portions of the wavelet transform, the neural network and fuzzy inference systems. This system uses a least-squares method as well as back-propagation methods to train the fuzzy inference system's membership function and its included parameters based on the wavelet-based filtered input and output data sets.

3.2.1. Takagi-Sugeno fuzzy model

Takagi-Sugeno (TS) fuzzy model is the backbone for the proposed WANFIS control system. In 1985, Takagi and Sugeno suggested an effective way for modeling complex nonlinear dynamic systems by introducing linear equations in consequent parts of a fuzzy model, which is called TS fuzzy model. It has led to reduction of computational cost because it does not need any defuzzification procedure. The fuzzy inference system used in the WANFIS model is of the TS fuzzy model form (Kim et al., 2009a). Typically, it takes the form of

$$R_j\text{: If } u_{FZ}^1 \text{ is } P_{1,j} \text{ and } u_{FZ}^2 \text{ is } P_{2,j} \ldots \text{and } u_{FZ}^i \text{ is } P_{i,j},$$
$$\text{Then } z = f_j\left(u_{FZ}^1, \ldots, u_{FZ}^i\right), \quad j = 1,2, \ldots, N_r, \tag{3-1}$$

where R_j is the j^{th} fuzzy rule, N_r is the number of fuzzy rule, $P_{i,j}$ are fuzzy sets centered at the j^{th} operating point, and u_{FZ}^i are premise variables that can be either input or output values. The

equation of the consequent part $z = f(u_{FZ}^1, \ldots, u_{FZ}^i)$ can be any linear equation. Note that the Eq. (1) represents the j^{th} local linear subsystem of a nonlinear system, i.e., a linear system model that is operated in only a limited region. All of the local subsystems are integrated by blending operating regions of each local subsystem using the fuzzy interpolation method as a global nonlinear system

$$y = \frac{\sum_{j=1}^{N_r} W_j(u_{FZ}^i)[f_j(u_{FZ}^1, \ldots, u_{FZ}^i)]}{\sum_{j=1}^{N_r} W_j(u_{FZ}^i)}, \tag{3-2}$$

where $W_j(u_{FZ}^i) = \prod_{i=1}^{n} \mu_{P_{i,j}}(u_{FZ}^i)$ and $\mu_{P_{i,j}}(u_{FZ}^i)$ is the grade of membership of u_{FZ}^i in$P_{i,j}$. These parameters are optimized by the back propagation neural network. A typical architecture of fuzzy rules is shown in figure 3-1, which shows four membership functions and sixteen rules, whereas the model in this paper uses only two membership functions and four rules.

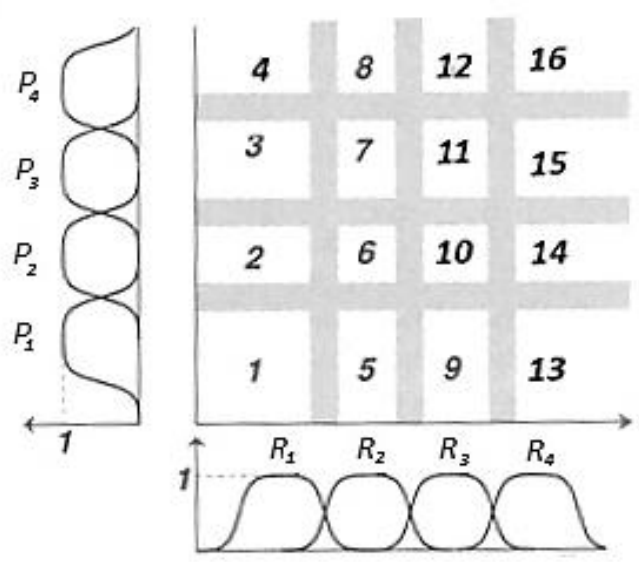

Figure 3-1. Typical fuzzy rules layout (Jang et al., 1997)

The main challenge in using a fuzzy model is the optimization of the parameters of the model. Therefore, incorporating neural networks to create an adaptive neuro-fuzzy inference system allows for these parameters to be optimized during computation, which is explained below.

3.2.2. ANFIS architecture

The architecture of an ANFIS model typically looks similar to figure 3-2.

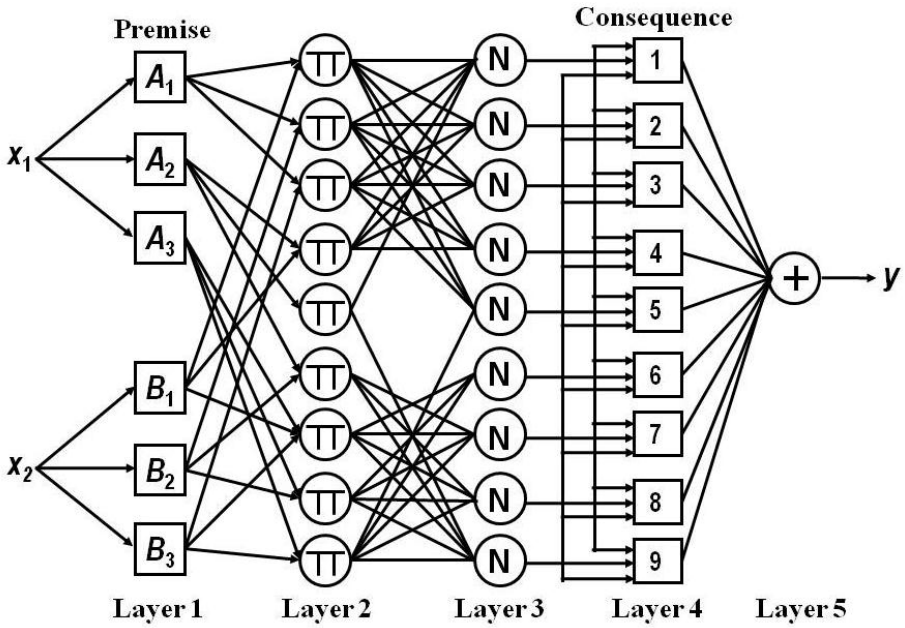

Figure 3-2. ANFIS architecture

This figure represents a two input, one output, and three membership functions (MF) system. Each layer has particular tasks to complete before the data moves to the next layer. In layer 1, the function of the node is represented by

$$F_{FZ}^{1,j} = \mu_{P_{i,j}}(u_{FZ}^{i}). \quad (3\text{-}3)$$

For a Gaussian MF used in this simulation,

$$\mu_{P_{i,j}}(u_{FZ}^{i}) = exp\left[-\frac{(u-a_1)^2}{2a_2^2}\right], \quad (3\text{-}4)$$

where a_1 and a_2 are adjustable parameters of the Gaussian function. This MF is applied to each input in layer 1. Layer 2 then outputs the product of all inputs into layer 2, known as the firing strength

$$F_{FZ}^{2,j} = \mu_{P_{i,j}}(u_{FZ}^{1}) \times \mu_{P_{i,j}}(u_{FZ}^{2}) \dots \mu_{P_{i,j}}(u_{FZ}^{i}). \quad (3\text{-}5)$$

Layer 3 takes a ratio of these layer 2 firing strengths in order to normalize the layer 2 outputs, such that

$$F_{FZ}^{3,j} = F_{FZ}^{2,j} / \sum_j \prod_{i=1}^{n} \mu_{P_{i,j}}(u_{FZ}^{i}). \quad (3\text{-}6)$$

Layer 4 then applies a node function to the normalized firing strengths

$$F_{FZ}^{4,j} = F_{FZ}^{3,j} * f_j = F_{FZ}^{3,j}\left[f_j(u_{FZ}^{1}, \dots, u_{FZ}^{i})\right], \quad (3\text{-}7)$$

where a_3, a_4, a_5 are function parameters for the consequent. The last layer summates the layer inputs

$$F_{FZ}^{5} = \frac{\sum_j \prod_{i=1}^{n} \mu_{P_{i,j}}(u_{FZ}^{i})[f_j(u_{FZ}^{1}, \ldots, u_{FZ}^{i})]}{\sum_j \prod_{i=1}^{n} \mu_{P_{i,j}}(u_{FZ}^{i})}. \quad (3\text{-}8)$$

The output of this system is then used in a hybrid learning algorithm to create a linear combination of the consequent parameters, a_3, a_4, a_5. The key parameters for this simulation include the number of iterations, or epochs, the number of MFs and the type of MF, as well as the step size of the function. Types of MFs can vary from a generalized bell function, Gaussian functions, sigmoidal functions, trapezoidal function, as well as other forms. Each change of variables will yield different output results (Jang, 1993; Yang and Lin, 2005). The fuzzy inference system sets up rules based on the number of MFs used in simulation. For a four MF system, the following fuzzy rules are set up and shown in figure 3-1. Each number represents one of the sixteen fuzzy regions that are created through the use of four MFs in the ANFIS model. The fuzzy region is defined by the premise, and the output is generated through the consequent.

Although the ANFIS is very effective in modeling complex nonlinear systems, it requires substantial computational loads. Such a problem can be addressed through the integration of wavelet transform-based multi-resolution analysis framework.

3.2.3. Wavelet transform

Wavelet analysis began during the 1980s by Morlet, who discovered the use of wavelet analysis in signal processing (Thuillard, 2001). It was created by modifying previous mathematical concepts such as Fourier analyses, where the time window is fixed to include the entirety of the signal. Wavelet theory began by bypassing this drawback of the Fourier analysis so that wavelet analysis used a variable time-window, allowing for scientists and engineers to look at a specific time frame of the signal for signal analysis. Mathematicians working with filter theory were able

to use this concept of wavelet analysis and apply it to their field, and reconstruction filters were developed. This meant that signals were able to be divided into sampled signals and then reconstructed into a signal that is equivalent to the original signal. Mallat (1989) created a fast wavelet decomposition algorithm to compute the wavelet coefficients using the wavelet filters, with one algorithm for decomposition of the signal and another algorithm for the reconstruction to the equivalent signal. Being able to reconstruct a signal using these algorithms provides the ability for data compression and noise reduction.

Fourier transforms and its modifications, such as short-time Fourier transforms and fast Fourier transforms, use a fixed time-frequency resolution, causing an issue in many engineering applications, mainly an inability to see low or high frequency portions of the window when viewing the entire window. A continuous wavelet transform was developed from the Fourier analysis, such that:

$$W_\Psi f(a,b) = 1/\sqrt{a} \int_{-\infty}^{\infty} f(x) * \Psi^* \left(\frac{x-b}{a}\right) dx, \quad \text{(3-9)}$$

where *a* is a scaling factor, *b* is the width of the window in the time domain, and Ψ is the wavelet function. From the continuous wavelet transform, the discrete wavelet transform can be derived, and is given as:

$$u_{FZ}^{i} = 2^{(s/2)} \sum_n x_i(n) \ \emptyset(2^s t - l), \quad \text{(3-10)}$$

and the original signal, $x(n)$, can be recalculated from the wavelet function using

$$x_i(n) = \sum_l \sum_s u_{FZ}^i \Psi_{l,s}(n). \quad (3\text{-}11)$$

Using discrete wavelet transforms allows for the isolation of high frequency components from the signal at the time they occur. This results in a signal of low frequency components with continuous magnitudes. In order to look at both high and low frequency portions of the signal, multi-resolution analysis should be investigated (Taha and Reda, 2004).

Multi-resolution analysis (MRA) was developed to decompose a function into slowly-varying and rapidly-varying segment signals, allowing for the divided function segments to be studied separately. This allows for a representation of the function at a single level of approximation by discretizing the function using the step size, and therefore significantly reducing the total number of data points needed to accurately represent the signal, which is also known as filtering the data signal. In essence, MRA decomposes a signal into multiple levels of resolution, or most commonly, into high frequency and low frequency resolutions. Studying the low frequency components provides the main features of the signal, while features of the high frequency resolution component can be useful in fields such as damage detection (Sharifi et al., (2011). The scaling function for the formulation of the wavelet transform in order to mathematically represent the MRA is

$$\emptyset_{l,s} := 2^{s/2}\emptyset(2^s t - l), \quad (3\text{-}12)$$

and the wavelet is given by

$$\Psi_{l,s} := 2^{s/2}\Psi(2^s t - l), \quad (3\text{-}13)$$

where l is the location index, s is the scale index, $\emptyset$ is the mother function, and Ψ is the scaling function. The scaling function is used to stretch or compress the function in the selected time domain. Any function $x_s(t)$ and $y_s(t)$ can be represented as the linear combination of $\emptyset_{l,s}(t)$

and $\Psi_{l,s}(t)$, respectively. The functions $x_{s-1}(t) \in A_{s-1}$ and $y_{s-1}(t) \in W_{s-1}$ are developed from $x_s \in A_s$, where W_s is called the wavelet subspace and is complimentary to A_s in A_{s+1} such that the intersection of A_s and W_s does not exist and the summation of A_s and W_s creates A_{s+1}. A typical graphical representation of this MRA is shown in figure 3-3.

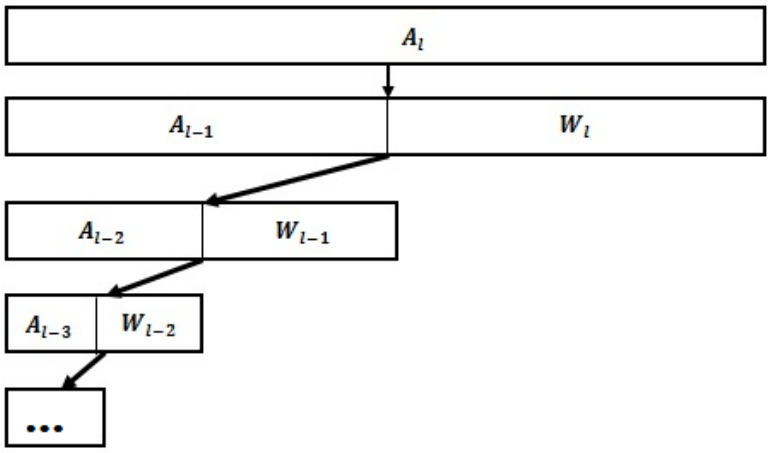

Figure 3-3. Wavelet transform-based multi-resolution analysis framework

3.2.4. Wavelet-based ANFIS control system

The inclusion of discrete wavelet transforms allow for an effective method to rid the control system of extraneous data, or noise. This methodology uses Daubechie filters for low frequency decomposition in order to de-noise response data that is then used as inputs to the ANFIS model. As mentioned earlier, the use of wavelet transforms allows for a fixed time-frequency resolution, meaning the window function is chosen, and then the resolution is fixed through processing. Representation of the function with several discretization steps allows for a reduction in the number of data points required for accurate representation of the system. This model proposes the use of two levels of discrete wavelet transforms as a means of filtering as well as applying

the ANFIS methodology to train to the control force of an optimal controller. The architecture of this proposed WANFIS system is depicted in figure 3-4.

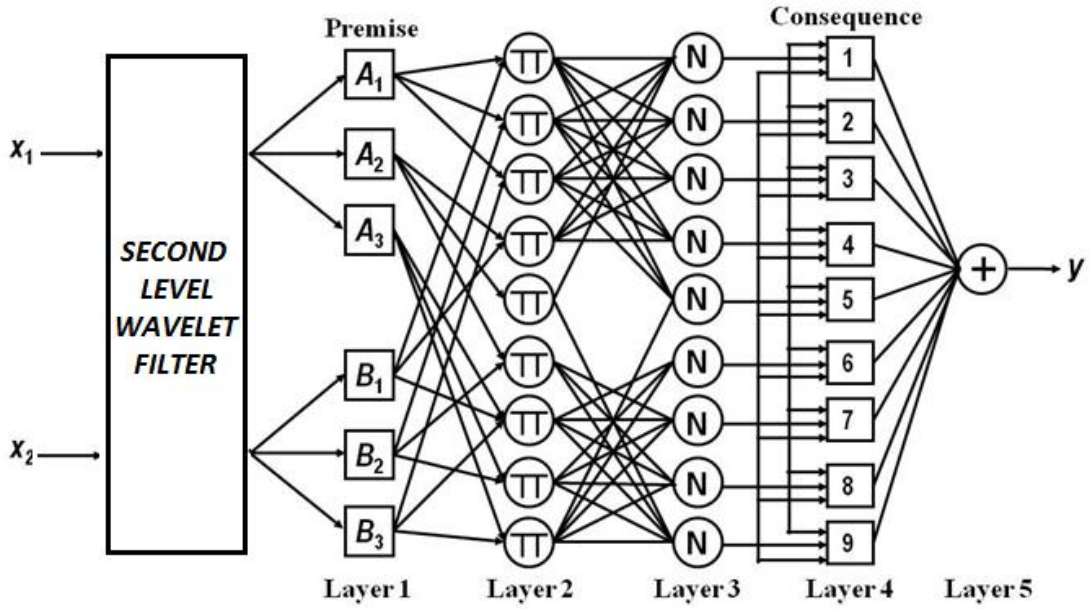

Figure 3-4. WANFIS architecture

The WANFIS algorithm is a two-input, one-output system to determine the control force of an actuator. For this study, the inputs to the WANFIS system were displacement and acceleration measurements. These were determined through an iterative process to maximize the results from training of the system, where velocity and drift responses were also studied to find the combination with the most favorable results.

The linear quadratic regulator (LQR) controller is first designed such that it guarantees the bounded input bounded output (BIBO) stability of the closed loop control system, and the WANFIS control system has been developed using a set of input and output data obtained from the LQR controller. It can be inferred that the proposed WANFIS control system can be BIBO stable if the WANFIS predicts the behavior of the LQR control system well. The proposed

control system can also be designed such that the structure system is globally asymptotically stable using parallel distribution compensation technique (Kim et al. 2009a). Next, simulations were performed on an eight-story building employing viscous fluid dampers and an active tuned mass damper to successfully reduce the seismic responses.

3.3. Example

To demonstrate the effectiveness of the wavelet-based adaptive neuro-fuzzy inference system (WANFIS) controller, an eight-story building structure equipped with passive fluid viscous dampers and an active tuned mass damper is investigated.

3.3.1. Building equipped with ATMD and viscous liquid dampers

In this study, an eight-story shear type building structure is investigated. The reason to choose this example is that it has been used as a benchmark problem by a number of researchers (Yang 1982; Yang et al. 1987; Soong 1990; Spencer et al. 1994; Kim et al. 2010b). The structure of interest is equipped with viscous fluid dampers located on each floor and an active tuned mass damper located on the eighth story. The associated equation of motion is given by

$$\mathbf{M}\ddot{x} + \mathbf{C}\dot{x} + \mathbf{K}x = \mathbf{\Gamma_a} \boldsymbol{f}_{\mathbf{a}}(t, \dot{x}_8, \ddot{x}_8) + \mathbf{\Gamma_d} \boldsymbol{f}_{\mathbf{d}}(\dot{x}_n)) - \mathbf{M\Lambda}\ddot{w}_g, \tag{3-14}$$

where $\boldsymbol{f}_{\mathbf{a}}$ and $\boldsymbol{f}_{\mathbf{d}}$ are the actuator and viscous liquid damper forces, respectively; $\ddot{w}_g$ denotes the ground acceleration, $\mathbf{M}$ the mass matrix, $\mathbf{K}$ the stiffness matrix, $\mathbf{C}$ the damping matrix, and the vector x the displacement relative to the ground, $\dot{x}$ the velocity, $\ddot{x}$ the acceleration; $\dot{x}_8$ and $\ddot{x}_8$ are the velocity and the acceleration at the 8^{th} floor level relative to the ground, respectively, $\dot{x}_n$ is the velocity at the n^{th} floor, and $\mathbf{\Gamma}$ and $\mathbf{\Lambda}$ are location vectors of control forces and disturbance

signal, respectively. This equation of motion and its relation to the building structure can be seen in figure 3-5.

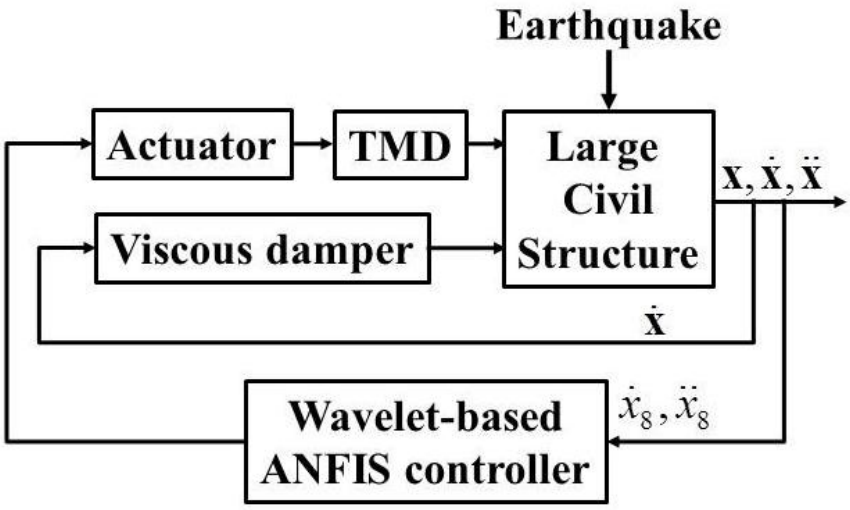

Figure 3-5. Configuration of the WANFIS feedback control system

The second order differential equation can be converted into a state space model

$$\begin{aligned} \dot{\boldsymbol{z}} &= \mathbf{A}\boldsymbol{z} + \mathbf{B}\boldsymbol{f}_{\mathbf{a}}(t, \dot{x}_8, \ddot{x}_8) + \mathbf{B}\boldsymbol{f}_{\mathbf{d}}(\dot{x}_n) - \mathbf{E}\ddot{w}_g \\ \boldsymbol{y} &= \mathbf{C}\boldsymbol{z} + \mathbf{D}\boldsymbol{f}_{\mathbf{a}}(t, \dot{x}_8, \ddot{x}_8) + \mathbf{D}\boldsymbol{f}_{\mathbf{d}}(\dot{x}_n) + \boldsymbol{n}, \end{aligned} \tag{3-15}$$

where

$$\mathbf{A} = \begin{bmatrix} 0 & \mathbf{I} \\ -\mathbf{M}^{-1}\mathbf{K} & -\mathbf{M}^{-1}\mathbf{C} \end{bmatrix} \tag{3-16}$$

$$\mathbf{B} = \begin{bmatrix} \mathbf{0} \\ \mathbf{M}^{-1}\mathbf{F} \end{bmatrix} \tag{3-17}$$

$$\mathbf{C} = \begin{bmatrix} \mathbf{I} & 0 \\ 0 & \mathbf{I} \\ -\mathbf{M}^{-1}\mathbf{K} & -\mathbf{M}^{-1}\mathbf{C} \end{bmatrix} \tag{3-18}$$

$$\mathbf{D} = \begin{bmatrix} 0 \\ 0 \\ \mathbf{M}^{-1}\mathbf{F} \end{bmatrix} \tag{3-19}$$

$$\mathbf{E} = \begin{bmatrix} 0 \\ \mathbf{F} \end{bmatrix} \tag{3-20}$$

F is the location matrix that locates Chevron braces within the building structure, and $\boldsymbol{n}$ is the noise vector. Properties of the eight-story building structure are adopted from (Yang et al., 2002).

3.3.2. Simulation

The simulations begin by determining the structural responses from an eight-story building structure of known parameters, shown in figure 3-6 along with the other control systems that a studied.

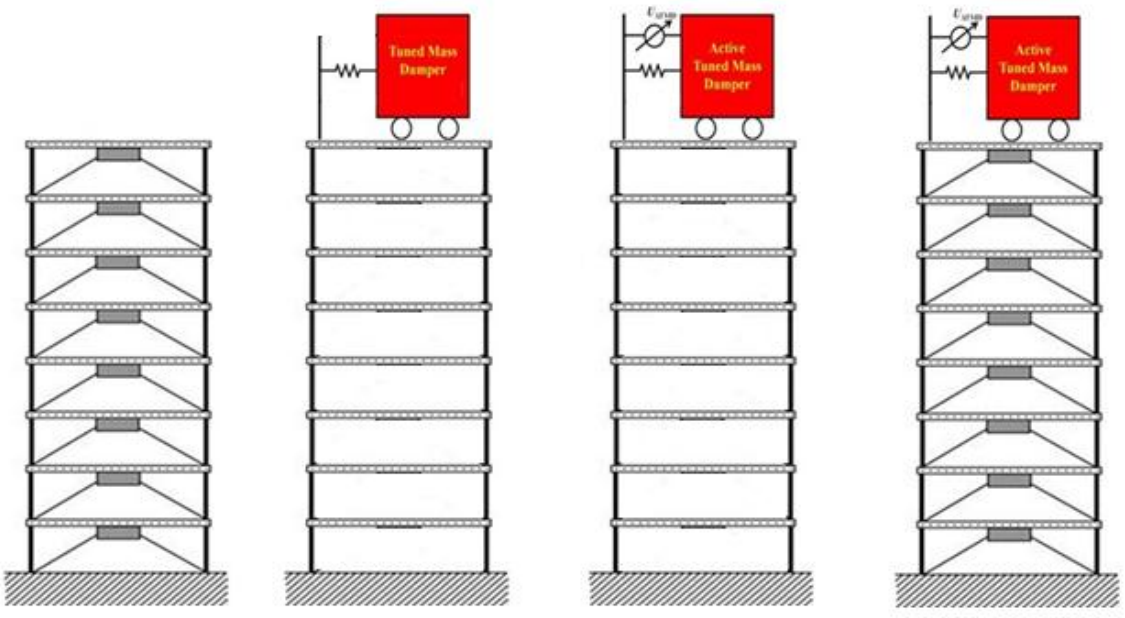

(a) Viscous damping (b) TMD system (c) ATMD system (d) Hybrid ATMD

Figure 3-6. Configuration of the 8-story building equipped with different control systems

The building is subjected to an artificial earthquake signal that incorporates aspects of the El-Centro, Kobe, Hachinohe, and Northridge earthquakes, shown in figure 3-7.

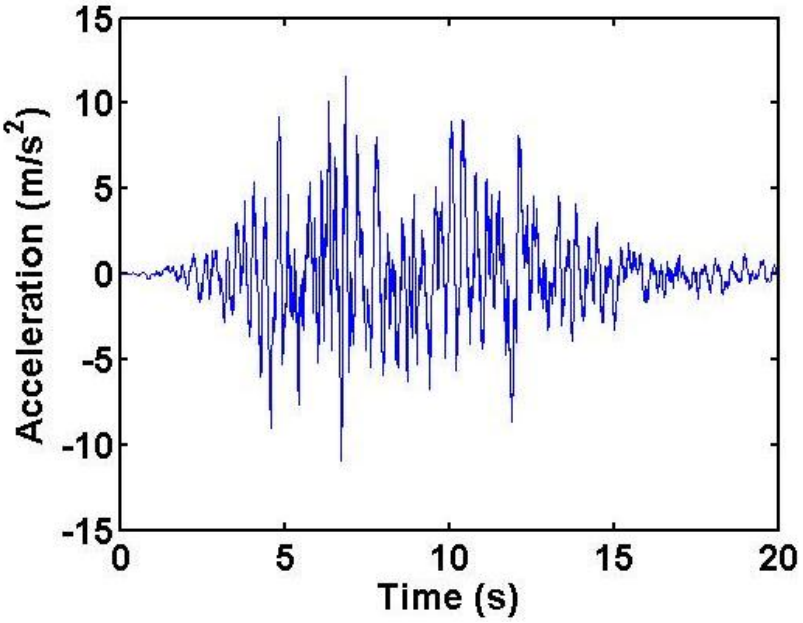

Figure 3-7. Artificial earthquake signal

Each floor of the eight-story building has the following structural properties: floor mass of 345,600 kg, internal stiffness of 340,400 kN/m, and internal damping coefficient of 2,937 tons/s.

The WANFIS controller is essentially used to emulate the performance of a full state feedback controller linear quadratic regulator (LQR) controller, without the use of all necessary sensors that the LQR requires. Creating the hybrid control system, the parameters of the active tuned mass damper (ATMD) were determined. This system was found to use an optimized mass of the TMD of 1.5% of the total mass of the structure, along with a stiffness of 0.47% of the structural stiffness of a floor. A normalization curve of the mass ratio is provided in figure 3-8.

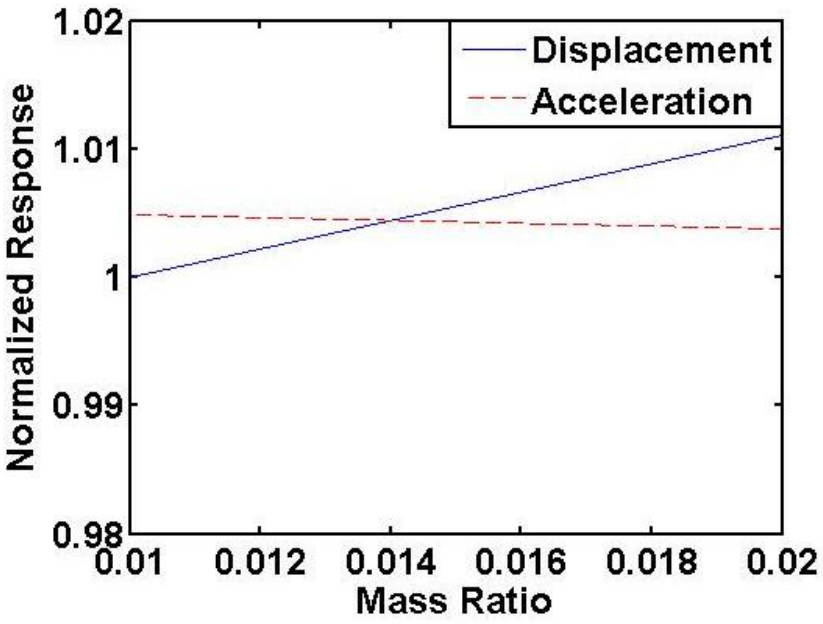

Figure 3-8. Mass ratio optimization of TMD

Using a genetic algorithm to determine the parameters of the TMD system was also explored (Cha and Kim 2012a-c). These parameters resulted in a mass ratio of 1.17%, along with a TMD stiffness of 1,214,217.877 kN/m and damping of 2,744.888 kN-s/m. However, it is noted that these parameters did not provide favorable results in the ATMD system, so the analytically optimized ATMD parameters of 1.5% of the total mass and 0.47% of the floor stiffness were used for simulations. From this, the WANFIS controller trained the input responses to the control force that would result from the use of the LQR controller. Membership functions prior to training and following training are provided in figure 3-9 to depict the training of the fuzzy model of the WANFIS system.

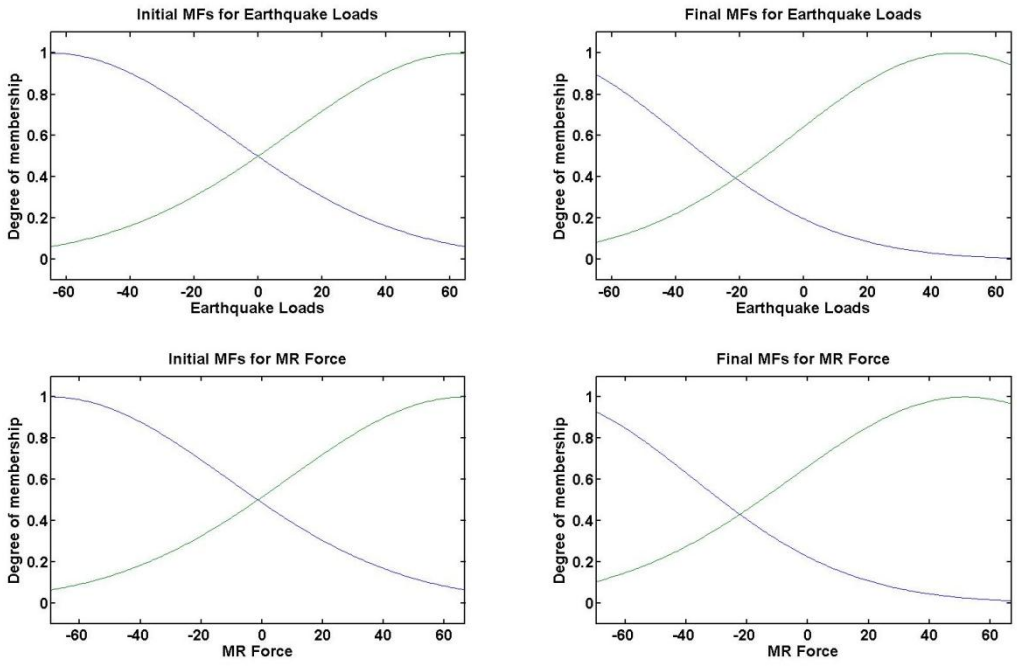

Figure 3-9. Membership functions before and after training

As mentioned previously, the WANFIS controller has an advantage over the ANFIS system in that it results in a smaller computation time. Table 3-1 provides the resulting eighth story displacement and acceleration responses of the ANFIS and WANFIS systems, including their computation times. Comparison to an ANFIS algorithm in the same control system and building resulted in a more reduced displacement and acceleration, as well as a computation time of 30.67 minutes for the ANFIS controller compared to 6.04 minutes for the WANFIS controller, successfully saving computation time while still maintaining comparable and adequate results. This structure resulted in an eighth-story displacement of 54.80 cm and an acceleration of 2330.2 cm/s^2 when no control system was employed, as well as a maximum interstory drift of 10.54 cm. As seen in Table 3-1, the WANFIS algorithm included in the hybrid control system provided an eighth-story displacement of 34.14 cm and an acceleration of 2177.8 cm/s^2, as well as a maximum interstory drift of 6.9 cm. Comparison to an LQR controller for the same building

resulted in a slightly greater eighth-story displacement and slightly lesser acceleration, but uses only two sensors compared to the necessary sixteen sensors required for an LQR controller to be used. Figures 3-10 and 3-11 provide time-history responses of the top floor, as well as the interstory responses of the structure.

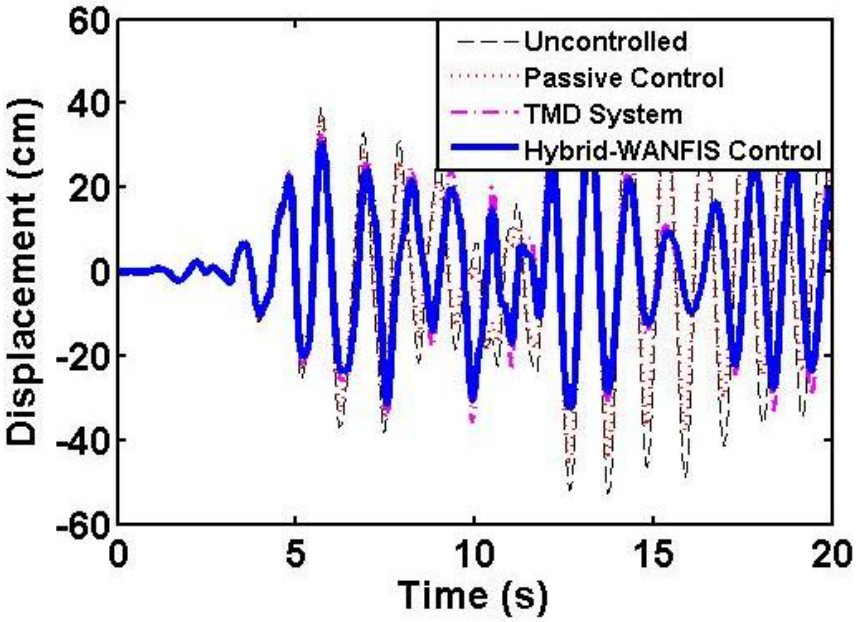

Figure 3-10. Time history responses: artificial earthquake

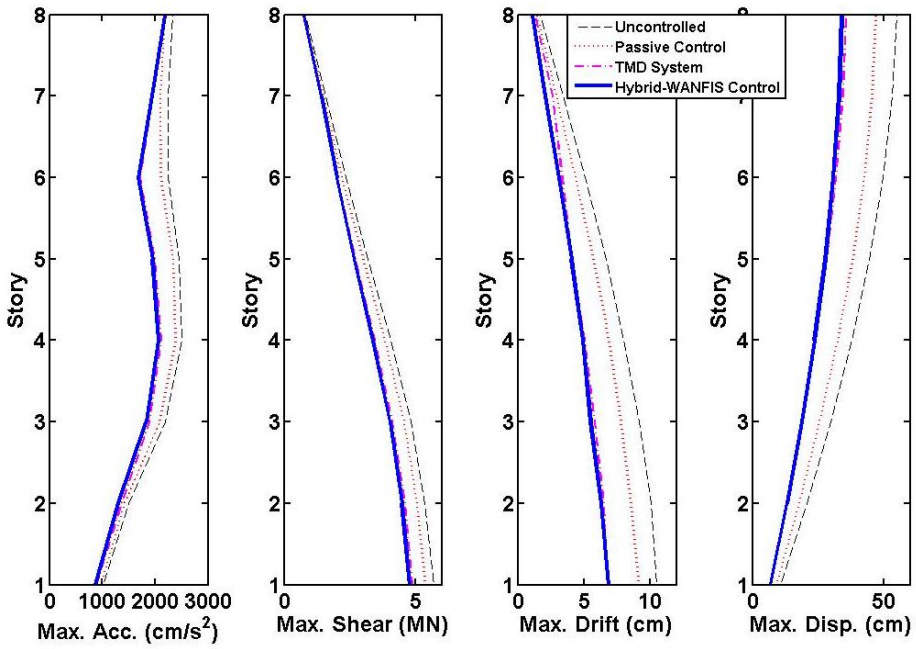

Figure 3-11. Maximum interstory responses: artificial earthquake

The proposed control system, WANFIS, is compared to an active and passive controller, as well as the uncontrolled response. It is shown from the figures that the proposed WANFIS control system is effective in reducing the seismic responses of high-rise building structures, which can be seen from the resulting values in Table 3-1.

Table 3-1. Performance comparison of ANFIS and WANFIS on the artificial earthquake

Hybrid Control System	Top Floor Responses		Training Time (sec)
	Displacement (cm)	Acceleration (cm/s^2)	
ANFIS	34.05	2179.0	1,840.2
WANFIS	34.14	2177.8	362.4

Validation of the WANFIS methodology was performed using the 1940 El-Centro earthquake, as well as signals of the Kobe, Hachinohe, and Northridge earthquakes. Figures 3-

12, 3-13, 3-14, and 3-15 provide the selected time-history response of eighth story displacement and the interstory responses of acceleration, shear, drift, and displacement for the El-Centro and Kobe earthquake signals.

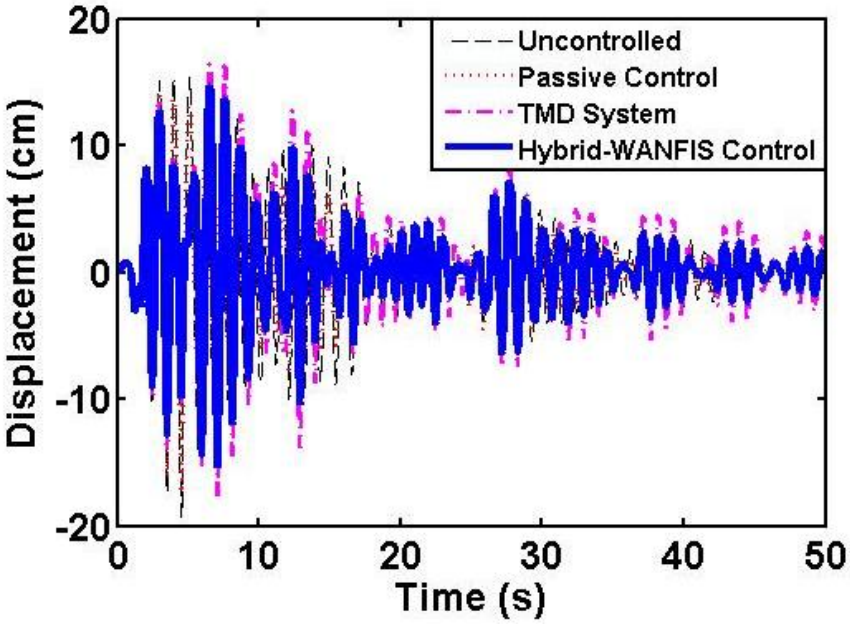

Figure 3-12. Time history responses: 1940 El-Centro earthquake

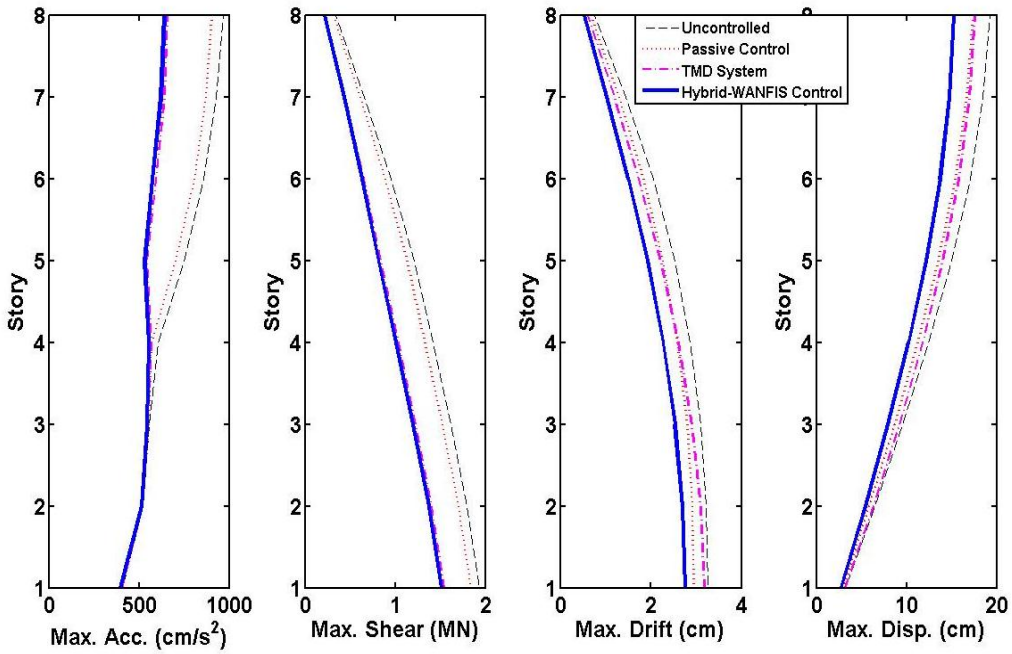

Figure 3-13. Maximum interstory responses: 1940 El-Centro earthquake

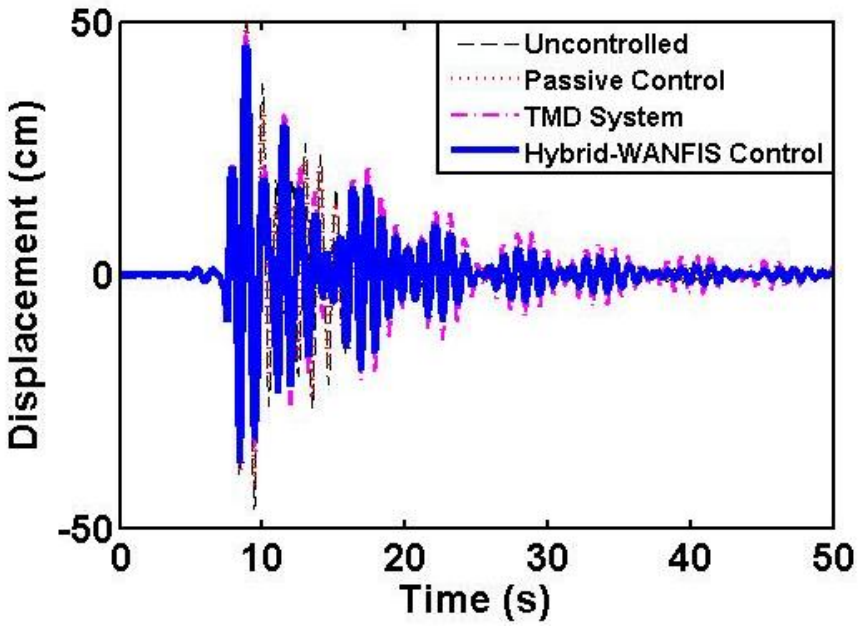

Figure 3-14. Time history responses: Kobe earthquake

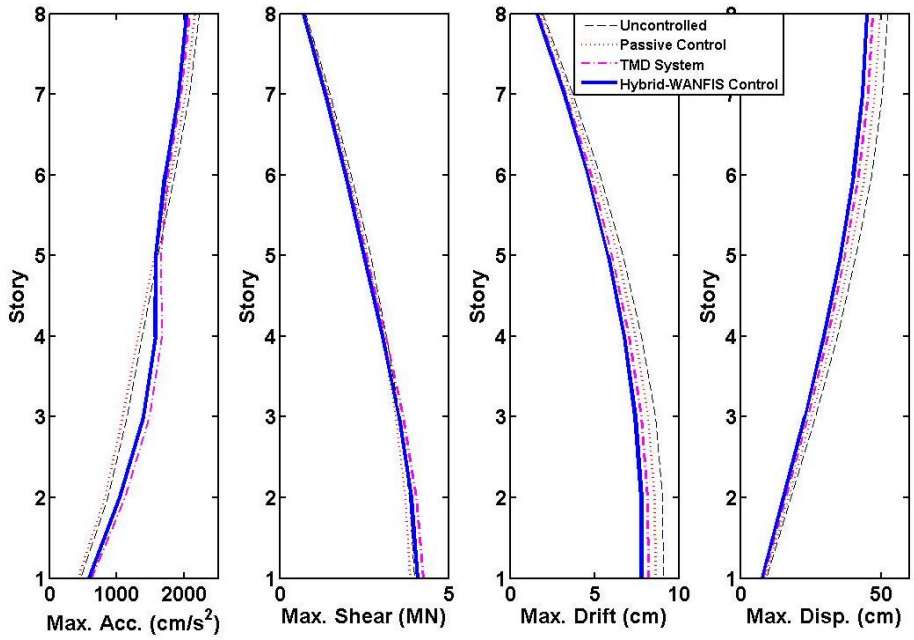

Figure 3-15. Maximum interstory responses: Kobe earthquake

To further determine the effectiveness of the proposed hybrid control system, performance criteria, presented by Spencer et al (1998), were used and detailed below. The results are provided in Table 3-2 for each of the earthquakes used for validation.

$$J_1 = max\left\{\frac{\max|x_i(t)|}{x_{u,max}}\right\} \tag{3-21}$$

$$J_2 = max\left\{\frac{\max(|d_i(t)|/h_i)}{d_{u,max}}\right\} \tag{3-22}$$

$$J_3 = max\left\{\frac{\max|\ddot{x}_i(t)|}{\ddot{x}_{u,max}}\right\} \tag{3-23}$$

$$J_4 = max\left\{\frac{\max|m_i\ddot{x}_i(t)|}{F_{b,max}}\right\} \tag{3-24}$$

$$J_5 = max\left\{\frac{\max\|x_i(t)\|}{\|x_{u,max}\|}\right\} \tag{3-25}$$

$$J_6 = max\left\{\frac{\max(\|d_i(t)\|/h_i)}{\|d_{u,max}\|}\right\} \tag{3-26}$$

$$J_7 = max\left\{\frac{\max\|\ddot{x}_i(t)\|}{\|\ddot{x}_{u,max}\|}\right\} \tag{3-27}$$

$$J_8 = max\left\{\frac{\max\|m_i\ddot{x}_i(t)\|}{\|F_{b,max}\|}\right\} \tag{3-28}$$

where $x_i(t)$ is the time history of displacement of the i^{th} floor of the control system, $x_{u,max}$ is the maximum displacement of the uncontrolled system, $|.|$ denotes the absolute value, $d_i(t)$ is the time history of drift of the i^{th} floor of the controlled system, h_i is the height of the i^{th} floor, $d_{u,max}$ is the maximum interstory drift of the uncontrolled system, $\ddot{x}_i(t)$ is the time history of acceleration of the i^{th} floor of the control system, $\ddot{x}_{u,max}$ is the maximum acceleration of the uncontrolled system, m_i is the mass of the i^{th} floor, $F_{b,max}$ is the maximum shear force of the uncontrolled system, and $\|.\|$ denotes the maximum normed value.

Table 3-2. Performance comparison of several control systems under a variety of earthquakes

Index		Artificial	El-Centro	Hachinohe	Northridge	Kobe	Ave.	Max
J_1	Dampers	0.8588	0.9031	**0.8686**	0.9703	0.9524	0.9106	0.9703
	TMD	0.6517	0.9151	0.9884	0.9925	0.9029	0.8901	0.9925
	WANFIS	**0.6229**	**0.7949**	0.8795	**0.9622**	**0.8637**	**0.8246**	**0.9622**
J_2	Dampers	0.8741	0.9064	0.8399	0.9645	0.9472	0.9064	0.9645
	TMD	**0.6476**	0.9802	0.9734	0.9735	0.9021	0.8954	0.9802
	WANFIS	0.6543	**0.8505**	**0.8326**	**0.9376**	**0.8581**	**0.8266**	**0.9376**
J_3	Dampers	0.9554	0.9320	**0.9745**	0.9842	0.9730	0.9638	0.9842
	TMD	0.8836	0.6802	1.0137	0.9674	0.9368	0.8963	1.0137
	WANFIS	**0.8698**	**0.6624**	0.9812	**0.9529**	**0.9164**	**0.8765**	**0.9812**
J_4	Dampers	0.9484	0.9528	**0.9730**	0.9763	**0.9656**	0.9632	**0.9763**
	TMD	0.8696	0.8002	1.0188	0.9795	1.0647	0.9446	1.0647
	WANFIS	**0.8390**	**0.7843**	0.9853	**0.9596**	1.0217	**0.9180**	1.0217
J_5	Dampers	0.8593	0.9040	**0.8493**	0.9675	0.9515	0.9063	0.9675
	TMD	0.6439	0.9299	0.9838	0.9806	0.9040	0.8884	0.9838
	WANFIS	**0.6251**	**0.8079**	0.8551	**0.9479**	**0.8640**	**0.8200**	**0.9479**
J_6	Dampers	0.8594	0.9038	**0.8508**	0.9670	0.9516	0.9065	0.9670
	TMD	0.6442	0.9284	0.9837	0.9799	0.9040	0.8880	0.9837
	WANFIS	**0.6257**	**0.8066**	0.8570	**0.9467**	**0.8641**	**0.8200**	**0.9467**
J_7	Dampers	0.9478	0.9482	**0.9738**	0.9780	**0.9687**	0.9633	**0.9780**
	TMD	0.8585	0.7781	1.0179	0.9779	1.0306	0.9326	1.0306
	WANFIS	**0.8384**	**0.7621**	0.9852	**0.9594**	0.9924	**0.9075**	0.9924
J_8	Dampers	0.9463	0.9458	**0.9744**	0.9787	**0.9688**	0.9628	**0.9797**
	TMD	0.8576	0.7596	1.0177	0.9779	1.0227	0.9271	1.0227
	WANFIS	**0.8387**	**0.7424**	0.9856	**0.9601**	0.9866	**0.9027**	0.9866

Using these indices, it is shown that the proposed WANFIS hybrid control system results in lower structural responses than the TMD system and passive control system for the artificial, El-Centro, Kobe, and Northridge earthquakes, as well as the lowest average index result for each of the eight indices taken into consideration. Through the values provided in Table 3-2, it can be seen that the displacement resulting from the proposed wavelet-based hybrid control system is an average of 9.44% and 7.36% lower than the passive and active control systems, respectively. Also, the accelerations of the hybrid control system are 9.06% and 2.20% lower than the passive and active control systems, respectively. Each index resulted in an average response lower than

that of the other two systems. It can also be shown from Table 3-2, the performance of Dampers is better than the proposed WANFIS control system in term of J_4, J_7, and J_8, which are functions of accelerations. The reason would be inferred from the fact that viscous liquid dampers do not input external energy to closed loop control system of a structure equipped with passive control devices, while an ATMD systems input an external energy generated by actuators to the structural system. Such energy can lead to increasing acceleration responses. However, it is noted that WANFIS system produces better performance than Dampers for most cases, excluding the cases listed above.

3.4. Conclusion

In this paper, a novel wavelet-based adaptive neuro-fuzzy inference system (WANFIS) is proposed for design of a hybrid control system for vibration control of buildings subject to earthquake loads. It is developed through the integration of neural networks, fuzzy logic theory, and wavelet transform algorithms. To train the WANFIS model, an artificial earthquake is used, which incorporated characteristics from various earthquake signals, while four different earthquake records are used to validate the developed model. To demonstrate the effectiveness of the proposed WANFIS control system, an eight-story building equipped with an actuator, a tuned mass damper, and passive viscous liquid dampers is investigated. It is shown from the simulation that the proposed control system uses use fewer sensors in the building than full state feedback controllers and also experiences less computation time than the ANFIS control algorithm with comparable resulting responses.

4. Active Control of Highway Bridge Under A Variety of Seismic Excitations

4.1. Introduction

With the continued deterioration of infrastructure in the United States, the need for healthy structures able to maintain their strength and serviceability throughout the length of their design life has become very important in structural engineering. Control systems can often be employed as a part of a structure in order to help the bridge or building act against lateral forces, such as strong wind and earthquake events. These events can vary greatly over time, creating a dynamic loading that may cause large, time-varying displacements, velocities, and accelerations on the structure, and these effects can impact the structure's health. The large structural responses can create or increase cracks and degrade the overall and local strength, eventually leading to damage or collapse.

Control systems are becoming increasingly researched and used on civil engineering structures to decrease and limit the responses of a building or bridge during a seismic event. Control systems utilize devices that apply a force to a structure that offsets internal forces, displacements, and accelerations that are created during seismic events. Two common forms of control systems are passive and active control. Passive control systems, such as viscous liquid dampers or base isolators, are devices designed and installed on a structure during construction, and implement a single control force during a dynamic loading event. Because they are installed during construction, it is very difficult and sometimes impossible to modify the device during the lifetime of a structure, but they are always on-line, always outputting a force when subjected to a loading. These devices are relatively inexpensive to design and implement, but are unable to

output a time-varying force during a dynamic event. Active control systems are time-dependent control devices, such as actuators and smart dampers. These devices are able to determine control forces in real-time, depending on the magnitude of the applied loadings on the structure. These systems are becoming more common, as being able to calculate actuator forces over time can provide much better results, since the force can increase as the loading increases.

Many control algorithms have been researched in the past, and the proposed algorithm, a wavelet-based adaptive neuro-fuzzy inference system (WANFIS), was created by combining discrete wavelet transforms with fuzzy logic theory and neural networks. The inclusion of wavelet transforms to the previously created ANFIS algorithm allows for a filtering of input data. The system will be detailed below.

The first model used as part of ANFIS and WANFIS systems is a fuzzy inference system (FIS). This system was developed through the use of fuzzy logic theory to create rules that the system follows. The FIS has a main advantage of being used as a nonparametric method for identification, and has been researched previously, including use in system identification (Zadeh, 1965; Takagi and Sugeno, 1985; Kim and Langari, 2007; Kim et al, 2009b; Kim et al, 2011), as well as general studies into the uncertainties and complexities due to the dynamic system (Langari, 1999; Kim et al, 2009a). Using a Takagi-Sugeno (TS) model for fuzzy logic theory allows for a representation of nonlinear systems using fuzzy rules and local linear models (Takagi and Sugeno, 1985; Yager and Filey, 1993; Johansen, 1994; Faravelli and Yao, 1996; Johansen and Babuška, 2003; Yan and Zhou, 2006; Chen et al, 2007; Du and Zhang, 2008; Kim et al 2010). One disadvantage of using fuzzy inference systems as a model is the optimization of parameters, which can be very complex and computationally intensive, leading itself to the inclusion of neural networks.

The use of a neural network is to develop a learning mechanism that emulates that of the human brain, such that it creates a network of interlinked nodes. These nodes, being connected, compute an output from the input to the node, and create a series of links between all nodes. As mentioned previously, the use of a fuzzy inference system can be complex and difficult in computations. Using a neural network in combination with a fuzzy inference system can create a model that is more efficient. The neural network adjusts parameters throughout the entirety of computation, which improve performances and decreases errors of the system. As it emulates the human brain and its cognitive mechanism, it is able to learn patterns and make adjustments as needed to further create a more improved model, and it has been studied previously to create a full model structure (Hung et al, 2003). However, due to the complexities of the neural networks, computation times can become excessive. Therefore, wavelet transforms can be used in conjunction with the combined fuzzy inference system and neural networks to filter input data and decrease computation times.

Wavelet transforms, combined with the ANFIS model, leads to the creation of a wavelet-filtered adaptive neuro-fuzzy inference system, or WANFIS. The wavelet transform can be used to filter out high or low frequency components from a data series. The wavelet transform improves upon previous methods due to its ability to incorporate an adjustable window function, allowing a user to analyze particular data points in a time series, rather than the entire time window, which is the case with Fourier transforms. Fourier transforms have been used previously for damage detection, system identification, and control systems, but require a fixed time-window for the entire data set. This can become difficult when analyzing data for long periods of time, as in the case in structural health monitoring, and can lead to missing key components, such as a particular damage point. The wavelet transform allows for an adjustable

window, and therefore provides an ability to look into any portion of a time series. Wavelet transforms can also be used as a means of filtering, which is critical in the use of the WANFIS model. As mentioned previously, the ANFIS system can require very long computation times due to the inclusion of neural networks and its ability to adjust and learn throughout the computation process. Being able to decrease the amount of data points while still maintaining the important components allows for a shorter computation time when compared to other systems. The proposed model uses two levels of discrete wavelet transforms for means of filtering data, which was optimized to create a balance between computation times and improved results.

The creation of the WANFIS system for means of structural control and control force algorithm is innovative in its application to control systems for mitigation of structural responses of civil engineering structures. Fuzzy logic controllers (Ahlawat and Ramaswamy, 2002) and ANDIS controllers (Hashim et al., 2004; Gu and Oyadiji, 2008) have been researched previously but the creation of the new WANFIS system should provide for decreased computation times while maintaining performance. This proposed control algorithm also requires less feedback information from the structure in comparison to full state feedback controllers, meaning less sensors are required to be installed on the structure, while reducing the structural responses in comparison with control systems. The next section will describe the WANFIS system, followed by simulation results showing the effectiveness of this system when subjected to seismic excitations.

4.2. Wavelet-based adaptive neuro-fuzzy inference system (WANFIS)

The WANFIS system incorporates a hybrid system to include portions of the wavelet transform, the neural network and fuzzy inference systems. This system uses a least-squares method as well as back-propagation methods to train the fuzzy inference system's membership functions and its included parameters based on the wavelet-based filtered input and output data sets.

4.2.1. Takagi-Sugeno fuzzy model

Takagi-Sugeno (TS) fuzzy model is the backbone for the proposed WANFIS control system. In 1985, Takagi and Sugeno suggested an effective means for modeling complex nonlinear dynamic systems by introducing linear equations in consequent parts of a fuzzy model, which is called TS fuzzy model. It has led to reduction of computational cost because it does not need any defuzzification procedure. The fuzzy inference system used in the WANFIS model is of the TS fuzzy model form (Kim et al., 2009a). Typically, it takes the form of

$$\begin{aligned} &R_j\text{: If } u_{FZ}^1 \text{ is } P_{1,j} \text{ and } u_{FZ}^2 \text{ is } P_{2,j} \ldots \text{and } u_{FZ}^i \text{ is } P_{i,j}, \\ &\text{Then } z = f_j\left(u_{FZ}^1, \ldots, u_{FZ}^i\right), \quad j = 1,2, \ldots, N_r, \end{aligned} \tag{4-1}$$

where R_j is the j^{th} fuzzy rule, N_r is the number of fuzzy rule, $P_{i,j}$ are fuzzy sets centered at the j^{th} operating point, and u_{FZ}^i are premise variables that can be either input or output values. The equation of the consequent part $z = f\left(u_{FZ}^1, \ldots, u_{FZ}^i\right)$ can be any linear equation. Note that the Eq. (4-1) represents the j^{th} local linear subsystem of a nonlinear system, i.e., a linear system model that is operated in only a limited region. All of the local subsystems are integrated by blending operating regions of each local subsystem using the fuzzy interpolation method as a global nonlinear system

$$y = \frac{\sum_{j=1}^{N_r} W_j(u_{FZ}^i)[f_j(u_{FZ}^1, \ldots, u_{FZ}^i)]}{\sum_{j=1}^{N_r} W_j(u_{FZ}^i)}, \tag{4-2}$$

where $W_j(u_{FZ}^i) = \prod_{i=1}^{n} \mu_{P_{i,j}}(u_{FZ}^i)$ and $\mu_{P_{i,j}}(u_{FZ}^i)$ is the grade of membership of u_{FZ}^i in$P_{i,j}$. These parameters are optimized by the back propagation neural network. A typical architecture of fuzzy rules is shown in figure 4-1, which shows four membership functions and sixteen rules, whereas the model in this paper uses only two membership functions and four rules.

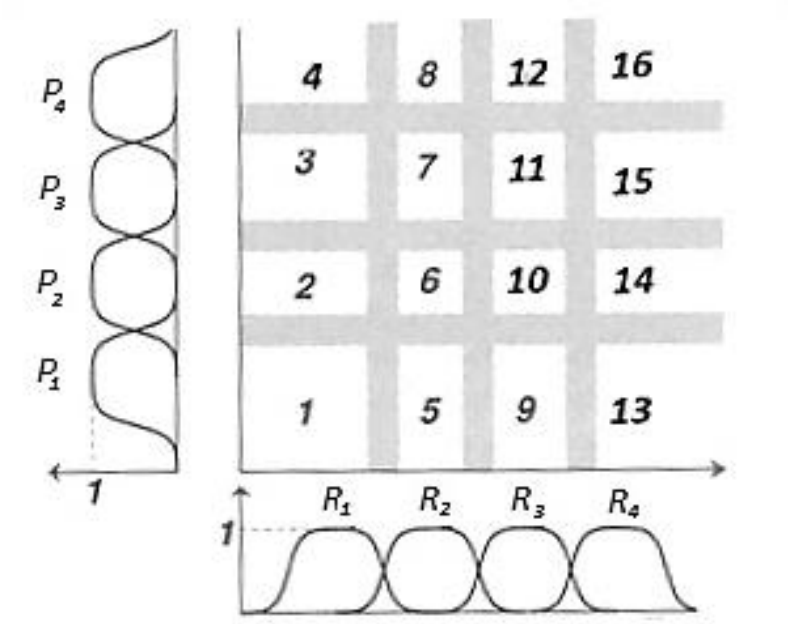

Figure 4-1. Typical fuzzy rules layout (Jang et al., 1997)

The main challenge in using a fuzzy model is the optimization of the parameters of the model. Therefore, incorporating neural networks to create an adaptive neuro-fuzzy inference system allows for these parameters to be optimized during computation, which is explained below.

4.2.2. ANFIS architecture

The architecture of an ANFIS model typically looks similar to figure 4-2.

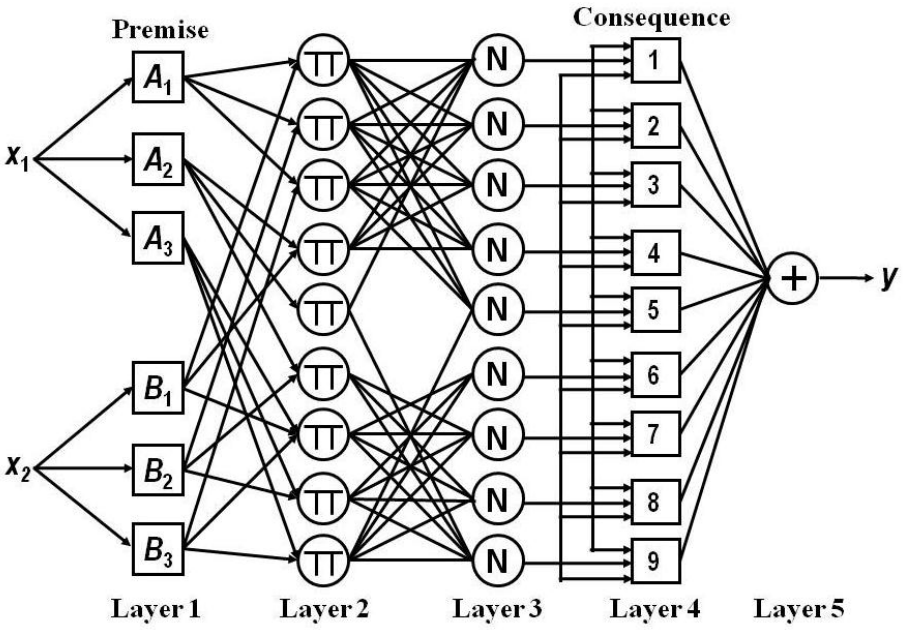

Figure 4-2. ANFIS architecture

This figure represents a two input, one output, and three membership functions (MF) system. Each layer has particular tasks to complete before the data moves to the next layer. In layer 1, the function of the node is represented by

$$F_{FZ}^{1,j} = \mu_{P_{i,j}}(u_{FZ}^{i}). \tag{4-3}$$

For a Gaussian MF used in this simulation,

$$\mu_{P_{i,j}}(u_{FZ}^{i}) = exp\left[-\frac{(u-a_1)^2}{2a_2^2}\right], \tag{4-4}$$

where a_1 and a_2 are adjustable parameters of the Gaussian function. This MF is applied to each input in layer 1. Layer 2 then outputs the product of all inputs into layer 2, known as the firing strength

$$F_{FZ}^{2,j} = \mu_{P_{i,j}}(u_{FZ}^{1}) \times \mu_{P_{i,j}}(u_{FZ}^{2}) \dots \mu_{P_{i,j}}(u_{FZ}^{i}). \quad (4\text{-}5)$$

Layer 3 takes a ratio of these layer 2 firing strengths in order to normalize the layer 2 outputs, such that

$$F_{FZ}^{3,j} = F_{FZ}^{2,j} / \sum_j \prod_{i=1}^{n} \mu_{P_{i,j}}(u_{FZ}^{i}). \quad (4\text{-}6)$$

Layer 4 then applies a node function to the normalized firing strengths

$$F_{FZ}^{4,j} = F_{FZ}^{3,j} * f_j = F_{FZ}^{3,j}\left[f_j(u_{FZ}^{1}, \dots, u_{FZ}^{i})\right], \quad (4\text{-}7)$$

where a_3, a_4, a_5 are function parameters for the consequent. The last layer summates the layer inputs

$$F_{FZ}^{5} = \frac{\sum_j \prod_{i=1}^{n} \mu_{P_{i,j}}(u_{FZ}^{i})\left[f_j(u_{FZ}^{1}, \dots, u_{FZ}^{i})\right]}{\sum_j \prod_{i=1}^{n} \mu_{P_{i,j}}(u_{FZ}^{i})}. \quad (4\text{-}8)$$

The output of this system is then used in a hybrid learning algorithm to create a linear combination of the consequent parameters, a_3, a_4, a_5. The key parameters for this simulation include the number of iterations, or epochs, the number of MFs and the type of MF, as well as the step size of the function. Types of MFs can vary from a generalized bell function, Gaussian functions, sigmoidal functions, trapezoidal function, as well as other forms. Each change of

variables will yield different output results (Jang, 1993; Yang and Lin, 2005). The fuzzy inference system sets up rules based on the number of MFs used in simulation. For a four MF system, the fuzzy rules are set up, and a generalized depiction is shown in figure 4-1. Each number represents one of the sixteen fuzzy regions that are created through the use of four MFs in the ANFIS model. The fuzzy region is defined by the premise, and the output is generated through the consequent.

Although the ANFIS is very effective in modeling complex nonlinear systems, it requires substantial computational loads. Such a problem can be addressed through the integration of wavelet transform-based multi-resolution analysis framework.

4.2.3. Wavelet transform

Wavelet analysis began during the 1980s by Morlet, who discovered the use of wavelet analysis in signal processing (Thuillard, 2001). It was created by modifying previous mathematical concepts such as Fourier analyses, where the time window is fixed to include the entirety of the signal. Wavelet theory enabled bypassing this drawback of the Fourier analysis through use of a variable time-window, allowing for scientists and engineers to look at a specific time frame of the signal for signal analysis. Mathematicians working with filter theory were able to use this concept of wavelet analysis and apply it to their field, and reconstruction filters were developed. This meant that signals were divisible into sampled signals and then reconstructed into a signal that is equivalent to the original signal. Mallat (1989) created a fast wavelet decomposition algorithm to compute the wavelet coefficients using the wavelet filters, with one algorithm for decomposition of the signal and another algorithm for the reconstruction to the equivalent signal.

The ability to reconstruct a signal using these algorithms provides the ability for data compression and noise reduction.

Fourier transforms and their modifications, such as short-time Fourier transforms and fast Fourier transforms, use a fixed time-frequency resolution, causing an issue in many engineering applications, mainly an inability to see low or high frequency portions of the window when viewing the entire window. A continuous wavelet transform was developed from the Fourier analysis, such that:

$$W_\Psi f(a,b) = 1/\sqrt{a}\int_{-\infty}^{\infty} f(x) * \Psi^*\left(\frac{x-b}{a}\right) dx, \quad \text{(4-9)}$$

where *a* is a scaling factor, *b* is the width of the window in the time domain, and Ψ is the wavelet function. From the continuous wavelet transform, the discrete wavelet transform can be derived, and is given as:

$$u_{FZ}^{i} = 2^{(s/2)}\sum_n x_i(n)\ \emptyset(2^s t - l). \quad \text{(4-10)}$$

The original signal, $x(n)$, can be recalculated from the wavelet function using

$$x_i(n) = \sum_l \sum_s u_{FZ}^{i} \Psi_{l,s}(n). \quad \text{(4-11)}$$

Using discrete wavelet transforms allows for the isolation of high frequency components from the signal at the time they occur. This results in a signal of low frequency components with continuous magnitudes. In order to look at both high and low frequency portions of the signal, multi-resolution analysis should be investigated (Taha and Reda, 2004).

Multi-resolution analysis (MRA) was developed to decompose a function into slowly-varying and rapidly-varying segment signals, allowing for the divided function segments to be

studied separately. This allows for a representation of the function at a single level of approximation by discretizing the function using the step size, and therefore significantly reducing the total number of data points needed to accurately represent the signal. This process is also known as filtering the data signal. In essence, MRA decomposes a signal into multiple levels of resolution, or most commonly, into high frequency and low frequency resolutions. Studying the low frequency components provides the main features of the signal, while features of the high frequency resolution component can be useful in fields such as damage detection (Sharifi et al., (2011). The scaling function for the formulation of the wavelet transform in order to mathematically represent the MRA is

$$\emptyset_{l,s} := 2^{s/2}\emptyset(2^s t - l), \tag{4-12}$$

and the wavelet is given by

$$\Psi_{l,s} := 2^{s/2}\Psi(2^s t - l), \tag{4-13}$$

where l is the location index, s is the scale index, $\emptyset$ is the mother function, and Ψ is the scaling function. The scaling function is used to stretch or compress the function in the selected time domain. Any function $x_s(t)$ and $y_s(t)$ can be represented as the linear combination of $\emptyset_{l,s}(t)$ and $\Psi_{l,s}(t)$, respectively. The functions $x_{s-1}(t) \in A_{s-1}$ and $y_{s-1}(t) \in W_{s-1}$ are developed from $x_s \in A_s$, where W_s is called the wavelet subspace and is complimentary to A_s in A_{s+1} such that the intersection of A_s and W_s does not exist and the summation of A_s and W_s creates A_{s+1}. A typical graphical representation of this MRA is shown in figure 4-3.

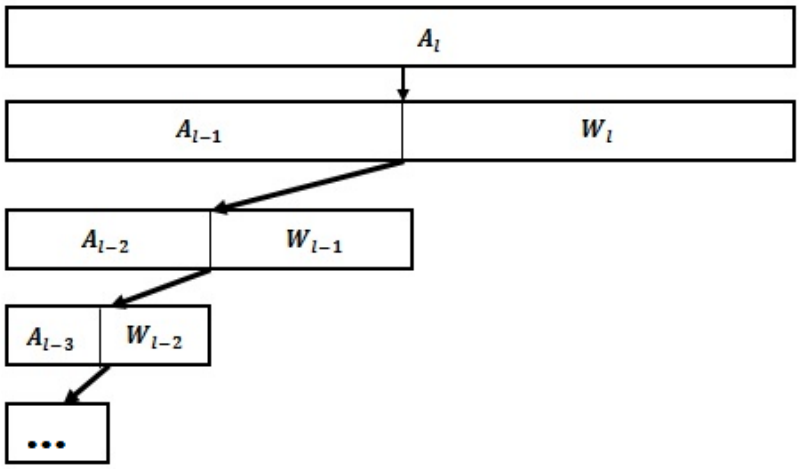

Figure 4-3. Wavelet transform-based multi-resolution analysis framework

4.2.4. Wavelet-based ANFIS control system

The inclusion of discrete wavelet transforms allow for an effective method to rid the control system of extraneous data, or noise. This methodology uses Daubechie filters for low frequency decomposition in order to de-noise response data that is then used as inputs to the ANFIS model. As mentioned earlier, the use of wavelet transforms allows for a fixed time-frequency resolution, meaning the window function is chosen, and then the resolution is fixed through processing. Representation of the function with several discretization steps allows for a reduction in the number of data points required for accurate representation of the system. This model proposes the use of two levels of discrete wavelet transforms as a means of filtering as well as applying the ANFIS methodology to train to the control force of an optimal controller, which creates an adequate balance between computation times and effective training of the model. The architecture of this proposed WANFIS system is depicted in figure 4-4.

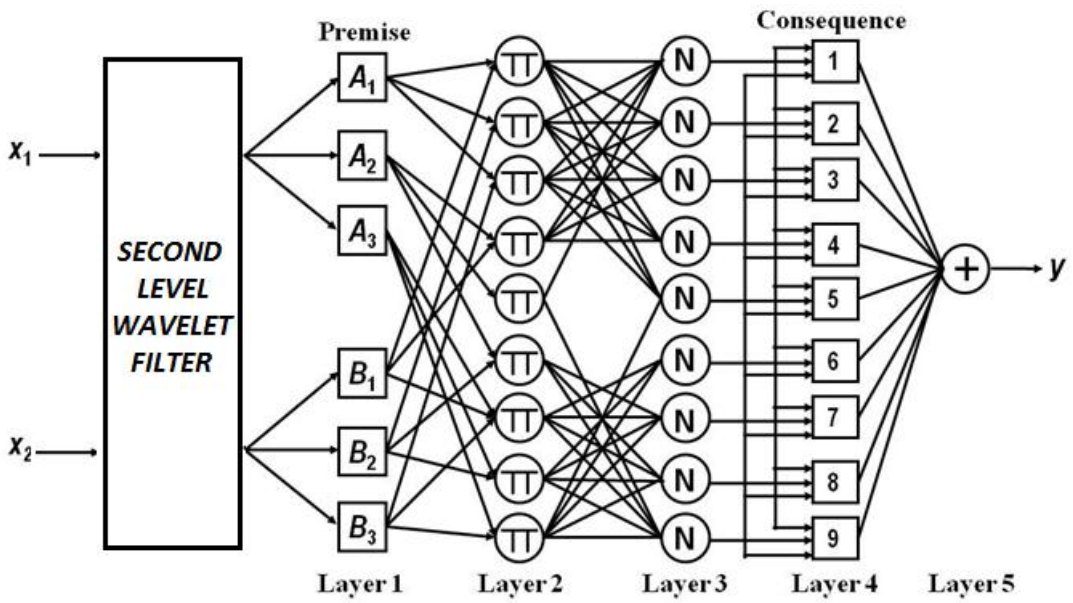

Figure 4-4. WANFIS architecture

The WANFIS algorithm is a two-input, one-output system to determine the control force of an actuator. For this study, the inputs to the WANFIS system were displacement and acceleration measurements. These were determined through an iterative process to maximize the results from training of the system, where velocity and drift responses were also studied to find the combination with the most favorable results. Next, simulations were performed on the benchmark highway bridge structure to successful reduce the seismic responses and improve the overall performance of the structure.

4.3. Example

The wavelet-based adaptive neuro-fuzzy inference system was tested on a benchmark highway bridge equipped with sixteen active control actuators to show its effectiveness in improving structural performance.

4.3.1. Benchmark Highway Bridge

To facilitate research in structural control, a benchmark bridge was developed based on an existing structure located at the crossing of the 91 and 5 highways in Orange County of California. The structure is a prestressed concrete box-girder, continuous over two spans of 58.5 m. The deck has a width of 12.95 m and 15 m for the east and west spans, respectively. The bridge carries four lanes of traffic atop columns of 6.9 m in height. The location of the bridge is within 20 km of two faults, the Whittier-Ellsinore and Newport-Inglewood fault zones, showing a great need for structural control due to its susceptibility to seismic events. This bridge has been described and researched previously (Agrawal et al, 2009). Figures 4-5 and 4-6 show the bridge schematic and finite element model.

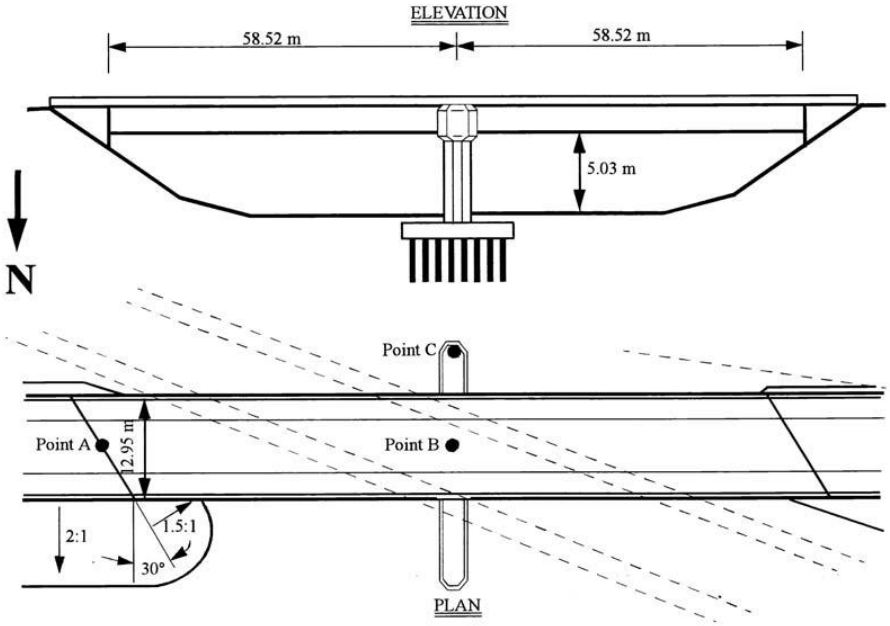

Figure 4-5. Benchmark highway bridge (Agrawal et al, 2009)

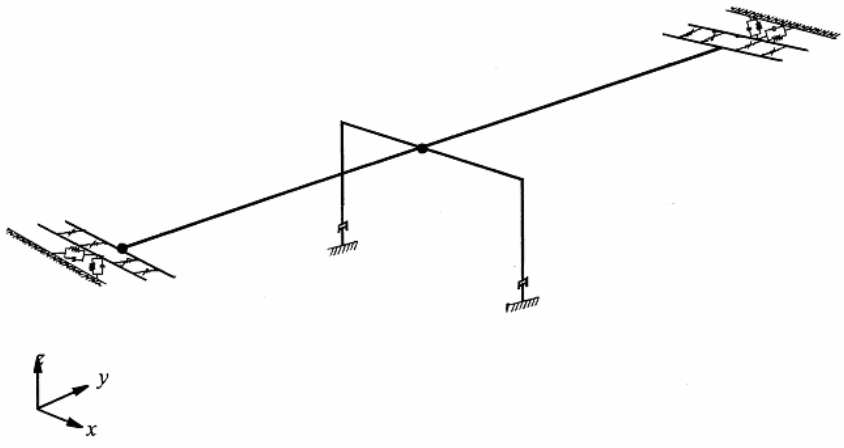

Figure 4-6. Finite element model of the highway bridge structure (Agrawal et al, 2009)

This bridge is equipped with sixteen actuators, with eight oriented in each the x- and y-directions. Figure 4-7 shows the feedback system for the bridge structure. This system shows the

simulation model, including the feedback of the states into the control devices, which are then forwarded back into the structure to reduce the structural responses.

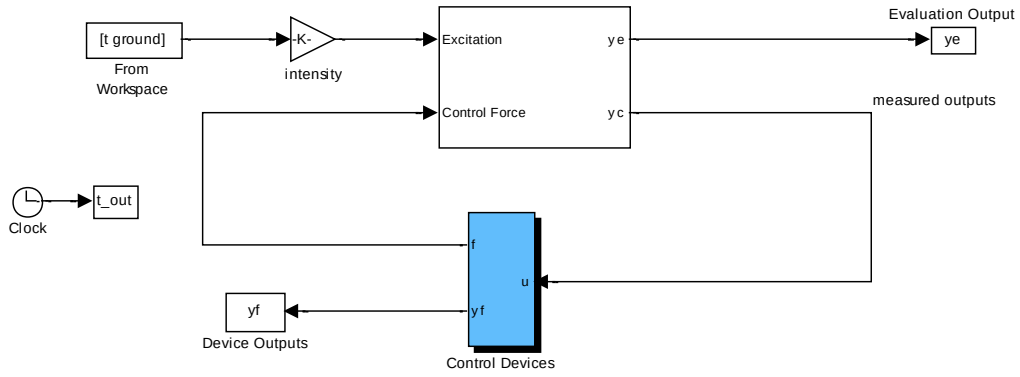

Figure 4-7. Control system architecture (Agrawal et al, 2009)

4.3.2. Simulation

The bridge structure of interest uses a benchmark linear quadratic Gaussian (LQG) control algorithm as a means for active control. This type of control is a variation of a linear quadratic regular, which is a full state feedback controller, but is able to reduce states to obtain comparable performance without needing full state feedback. The simulations began by determining the control force developed for an LQG control model, and using the WANFIS controller to train to the LQG control forces. An artificial earthquake was developed to train the WANFIS model for, which encompassed aspects of all six validating earthquakes: Turkey Bolu, Northridge, North Palm Springs, El-Centro, Rinadi, and Kobe. This artificial earthquake was used to determine the control forces, and then the WANFIS model was used to train to these control forces. The artificial earthquake signal is provided in figure 4-8.

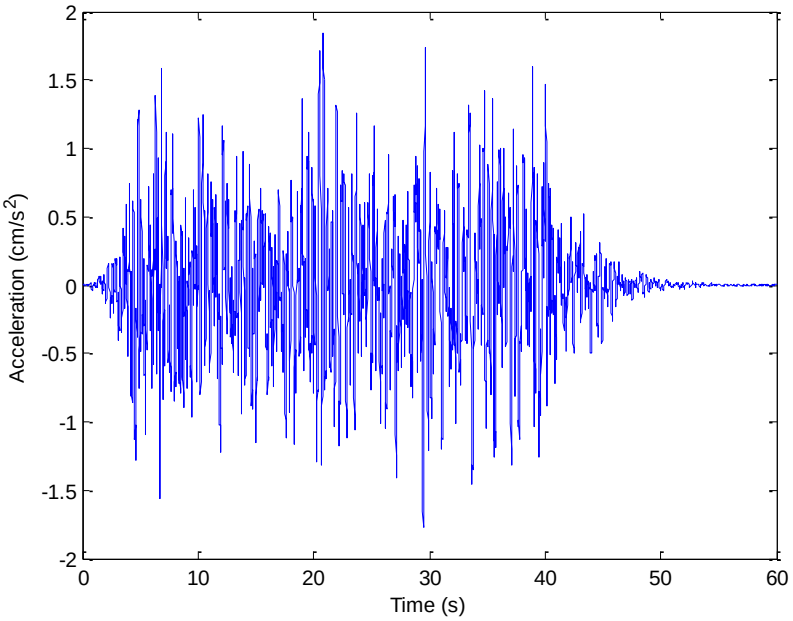

Figure 4-8. Artificial earthquake signal

From there, simulations using the WANFIS system and provided feedback system were performed to determine the best arrangement of control forces and actuators. It was found that the computation of only two control forces would be needed to calculate, one for all eight actuators oriented in the x-direction, and one for all eight actuators oriented in the y-direction. This set up was compared to using sixteen control forces, one for each individual actuator, and was found to yield more favorable results while using less power output and control force magnitudes. The training time for this model results in 187 seconds, or 3.12 minutes for a 4-Gaussian membership function model. The resulting membership functions of this training are depicted in figure 4-9.

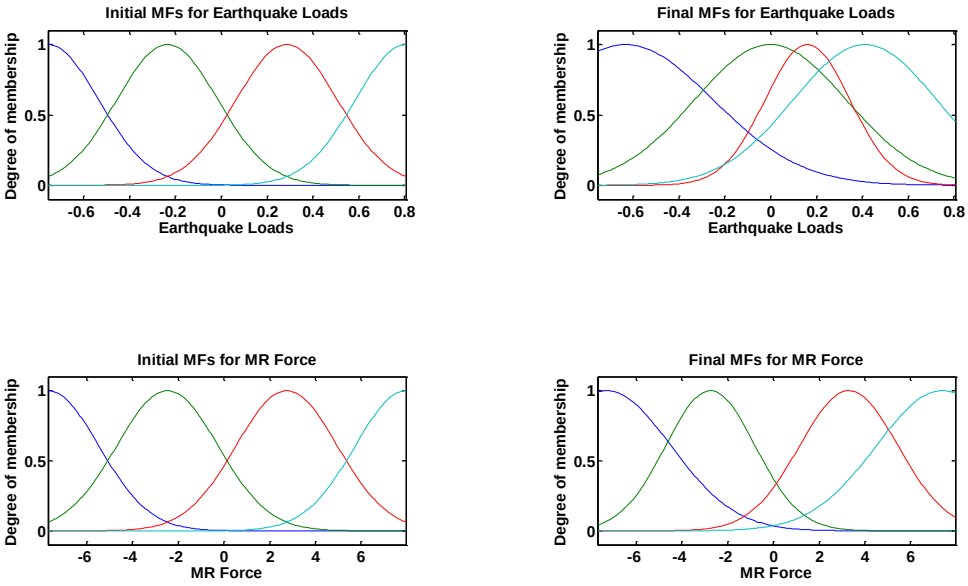

Figure 4-9. Membership functions before and after training

Another WANFIS model was examined, using the algorithm to train to the control forces from a genetic algorithm (Cha and Angrawal, 2011). It was found through simulations that using this differing control algorithm, the same set up as previously used could be used. This set up, described above, used only two control actuator forces, one in the x- and y-directions. The training time for this model results in 1368 seconds, or 22.8 minutes for each control force, using a 4-Gaussian membership function model.

As a means of validation and comparison, indices provided through the benchmark bridge structure were used. These indices compare structural responses and control outputs of the proposed system to that of the uncontrolled structure, showing how much each index was reduced. These indices are detailed below, and Table 4-1 provides

$$J_1 = max\left\{\frac{\max|F_{bi}(t)|}{F_{0b,max}}\right\} \tag{4-14}$$

$$J_2 = max\left\{\frac{\max(|M_{bi}(t)|)}{M_{0b,max}}\right\} \tag{4-15}$$

$$J_3 = max\left\{\frac{\max|y_{mi}(t)|}{y_{0m,max}}\right\} \tag{4-16}$$

$$J_4 = max\left\{\frac{\max|\ddot{y}_{mi}(t)|}{\ddot{y}_{0m,max}}\right\} \tag{4-17}$$

$$J_5 = max\left\{\frac{\max|y_{bi}(t)|}{|y_{0b,max}|}\right\} \tag{4-18}$$

$$J_6 = max\left\{\frac{\max(|\Phi_i(t)|)}{\Phi_{max}}\right\} \tag{4-19}$$

$$J_7 = max\left\{\frac{\max\int dE_i}{E_{max}}\right\} \tag{4-20}$$

$$J_8 = max\left\{\frac{N_{c,d}}{N_d}\right\} \tag{4-21}$$

$$J_9 = max\left\{\frac{\max\|F_{bi}(t)\|}{\|F_{0b,max}\|}\right\} \tag{4-22}$$

$$J_{10} = max\left\{\frac{\max(\|M_{bi}(t)\|)}{\|M_{0b,max}\|}\right\} \tag{4-23}$$

$$J_{11} = max\left\{\frac{\max\|y_{mi}(t)\|}{\|y_{0m,max}\|}\right\} \tag{4-24}$$

$$J_{12} = max\left\{\frac{\max\|\ddot{y}_{mi}(t)\|}{\|\ddot{y}_{0m,max}\|}\right\} \tag{4-25}$$

$$J_{13} = max\left\{\frac{\max\|y_{bi}(t)\|}{\|y_{0b,max}\|}\right\} \tag{4-26}$$

$$J_{14} = max\left\{\frac{\max(\|\Phi_i(t)\|)}{\|\Phi_{max}\|}\right\} \tag{4-27}$$

$$J_{15} = max\left\{\max(\frac{f_l(t)}{W})\right\} \tag{4-28}$$

$$J_{16} = max\left\{\max(\frac{d_l(t)}{x_{0m,max}})\right\} \tag{4-29}$$

$$J_{17} = max\left\{\frac{\max[\sum_l P_l(t)]}{\dot{x}_{0m,max}W}\right\} \tag{4-30}$$

$$J_{18} = max\left\{\frac{\max\left[\sum_l \int_0^{t_f} P_l(t)\right]}{x_{0m,max}W}\right\} \tag{4-31}$$

$$J_{19} = \text{number of control devices} \tag{4-32}$$

$$J_{20} = \text{number of required sensors} \tag{4-33}$$

$$J_{21} = \dim(x_{c,k}) \tag{4-34}$$

where $F_{bi}(t)$ is the time history of shear force of the i^{th} degree of freedom of the control system, $F_{0b,max}$ is the maximum shear force of the uncontrolled structure, $M_{bi}(t)$ is the time history of overturning moment, $M_{0b,max}$ is the maximum overturning moment of the uncontrolled structure, $y_{mi}(t)$ is the time history of the midspan displacement, $y_{0m,max}$ is the maximum midspan displacement of the uncontrolled structure, $|\ddot{y}_{mi}(t)|$ is the time history of the midspan acceleration, $\ddot{y}_{0m,max}$ is the maximum acceleration of the uncontrolled structure, $y_{bi}(t)$ is the time history of the abutment displacement, $y_{0b,max}$ is the maximum abutment displacement of the uncontrolled structure, $\Phi_i(t)$ is the time history of the ductility, Φ_{max} is the maximum ductility of the uncontrolled structure, $dE_i$is the dissipated energy of curvature at the column, E_{max} is the maximum dissipated energy of the curvature at the column of the uncontrolled structure, $N_{c,d}$ is the number of plastic connections of the control system, N_d is the number of plastic connections of the uncontrolled system, $|.|$ denotes the absolute value, $\|.\|$ denotes the

normalized value, $f_l(t)$ is the time history of the control force from the control device, W is the seismic weight of the system, $d_l(t)$ is the stroke of the control device, $x_{0m,max}$ is the maximum bearing deformation of the uncontrolled system, $P_l(t)$ is the time history of the instantaneous power required for the control device, $\dot{x}_{0m,max}$ is the maximum velocity of bearing of the uncontrolled system, and $x_{c,k}$ is the discrete state vector for the control algorithm (Agrawal et al, 2009).

Using these indices, it is shown that the proposed WANFIS control algorithms results in lower structural responses than the benchmark LQG control algorithm for the artificial, El-Centro, Kobe, North Palm Springs, Turkey Bolu and Rinadi earthquakes. The system as a whole improved the performance on 68% of the indices when training to the LQG control force, and 62% of the indices when training to the genetic algorithm. The LQG-trained model improved 67% of the average index values, and the genetic algorithm-trained model improved 57% of the average index values.

4.4. Conclusion

This paper proposes a wavelet-based adaptive neuro-fuzzy inference system (WANFIS) as a means for active control of bridge structures. This system combines aspects of discrete wavelet transforms, neural networks, and fuzzy logic theory. The WANFIS system is trained using an artificial earthquake, which combines aspects of various earthquake accelerations. This system is shown to be effective in reducing structural responses of a benchmark highway bridge equipped with sixteen control actuators, while also reducing the power output, control force magnitude,

and the required number of sensors installed on the bridge. The system also greatly reduces computation time of control forces in comparison with other control algorithms.

INDEX	Npalmspr			ChiChi			ElCentro			Rinadi			TurkBolu			Kobe			Ave.			Max.		
	LQG	WANFIS-LQG	WANFIS-GA	LQG	WANFIS-LQG	WANFIS-GA	LQG	WANFIS-LQG	WANFIS-GA	LQG	WANFIS-LQG	WANFIS-GA	LQG	WANFIS-LQG	WANFIS-GA	LQG	WANFIS-LQG	WANFIS-GA	LQG	WANFIS-LQG	WANFIS-GA	LQG	WANFIS-LQG	WANFIS-GA
J_1	0.95	**0.92**	0.96	0.88	**0.85**	**0.74**	0.79	0.86	0.80	0.90	**0.87**	**0.78**	0.91	**0.89**	**0.90**	0.79	0.84	0.89	0.85	0.87	**0.85**	0.95	**0.92**	0.96
J_2	0.77	**0.76**	0.80	0.97	**0.97**	**0.96**	0.74	0.79	**0.73**	0.98	**0.98**	**0.96**	0.98	0.98	0.98	0.70	**0.67**	0.78	0.86	0.86	0.87	0.98	0.98	0.98
J_3	0.82	**0.82**	**0.82**	0.80	**0.78**	**0.68**	0.78	0.87	0.80	0.87	**0.84**	**0.71**	0.75	**0.74**	**0.72**	0.70	**0.66**	0.79	0.79	**0.79**	**0.75**	0.87	0.87	**0.82**
J_4	0.79	0.93	0.94	0.88	0.90	0.98	0.88	0.96	1.00	0.84	0.90	0.98	0.80	0.81	0.91	0.90	0.95	0.94	0.85	0.91	0.96	0.90	0.96	1.00
J_5	0.94	**0.83**	**0.82**	0.80	**0.77**	**0.64**	0.64	0.69	**0.46**	0.88	**0.83**	**0.68**	0.71	0.72	**0.69**	0.59	0.61	**0.45**	0.76	**0.74**	**0.62**	0.94	**0.83**	**0.82**
J_6	0.77	0.76	0.80	0.74	**0.70**	**0.56**	0.74	0.79	**0.73**	0.85	**0.79**	**0.61**	0.46	**0.46**	**0.36**	0.70	**0.67**	0.78	0.71	**0.70**	**0.64**	0.85	**0.79**	**0.80**
J_7	0	0	0	0.51	**0.44**	**0.35**	0	0	0	0.62	**0.50**	**0.39**	0.33	**0.25**	**0.11**	0	0	0	0.24	**0.20**	**0.14**	0.62	**0.50**	**0.39**
J_8	0	0	0	0.67	**0.67**	**0.67**	0	0	0	1.00	**1.00**	**1.00**	0.33	**0.33**	**0.33**	0	0	0	0.33	0.33	0.33	1.00	1.00	1.00
J_9	0.74	0.79	0.80	0.89	**0.86**	**0.84**	0.68	0.69	0.72	0.87	**0.82**	**0.80**	0.89	**0.89**	**0.84**	0.71	**0.73**	0.79	0.80	**0.80**	**0.80**	0.89	**0.89**	**0.84**
J_{10}	0.70	0.71	0.74	0.83	**0.81**	**0.79**	0.64	0.65	0.69	0.88	**0.82**	**0.82**	0.53	0.59	**0.48**	0.61	**0.70**	0.75	0.70	0.71	0.71	0.88	**0.82**	**0.82**
J_{11}	0.70	0.73	0.75	0.78	**0.78**	**0.70**	0.66	0.66	0.71	0.80	**0.77**	**0.70**	0.61	0.62	**0.56**	0.73	**0.72**	0.77	0.71	**0.71**	**0.70**	0.80	**0.78**	**0.77**
J_{12}	0.72	0.92	0.86	0.79	0.81	0.85	0.69	0.73	0.80	0.80	0.80	0.84	0.79	0.87	0.88	0.80	0.85	0.88	0.77	0.83	0.85	0.80	0.92	0.88
J_{13}	0.48	**0.43**	**0.37**	0.78	**0.78**	**0.67**	0.48	0.60	**0.46**	0.82	**0.77**	**0.68**	0.52	**0.45**	**0.42**	0.47	**0.47**	**0.41**	0.59	**0.58**	**0.50**	0.82	**0.78**	**0.68**
J_{14}	0.70	0.71	0.74	0.65	0.79	**0.38**	0.64	0.65	0.69	0.83	0.86	**0.58**	0.24	0.38	**0.12**	0.71	**0.70**	0.75	0.63	0.68	**0.54**	0.83	0.86	**0.75**
J_{15}	0.01	**0.01**	0.01	0.02	**0.02**	0.03	0.01	**0.01**	0.01	0.02	**0.02**	0.03	0.01	**0.01**	0.02	0.01	0.01	0.01	0.01	**0.01**	0.02	0.02	**0.02**	0.03
J_{16}	0.90	**0.79**	**0.79**	0.77	**0.74**	**0.62**	0.59	0.63	**0.42**	0.80	**0.76**	**0.62**	0.71	0.71	**0.69**	0.51	0.60	**0.44**	0.71	**0.71**	**0.60**	0.90	**0.79**	**0.79**
J_{17}	0.05	**0.04**	**0.05**	0.11	**0.11**	0.16	0.02	**0.02**	0.03	0.11	**0.10**	0.12	0.07	**0.06**	0.08	0.07	**0.03**	**0.03**	0.07	**0.06**	0.08	0.11	**0.11**	0.16
J_{18}	0.01	**0.01**	**0.01**	0.02	**0.02**	0.02	0.00	**0.00**	0.00	0.02	**0.01**	0.02	0.01	**0.01**	0.02	0.01	**0.01**	**0.01**	0.01	**0.01**	0.01	0.02	**0.02**	**0.02**
J_{19}	16	16	16	16	16	16	16	16	16	16	16	16	16	16	16	16	16	16	16	16	16	16	16	16
J_{20}	12	**4**	**4**	12	**4**	**4**	12	**4**	**4**	12	**4**	**4**	12	**4**	**4**	12	**4**	**4**	12	**4**	**4**	12	**4**	**4**
J_{21}	28	**20**	**20**	28	**20**	**20**	28	**20**	**20**	28	**20**	**20**	28	**20**	**20**	28	**20**	**20**	28	**20**	**20**	28	**20**	**20**

Table 4-1. Performance comparison of WANFIS control systems to benchmark control under a variety of earthquakes

5. Summary

The proposed wavelet-based adaptive neuro-fuzzy inference system combines aspect of fuzzy logic theory, neural networks, and wavelet transforms to create a new system to be applied to civil engineering structures. The system benefits from being robust against uncertainties, while reducing computation times of previous algorithms. Two aspects of structural health monitoring shown that this model is shown to be effective for are system identification and structural control. The WANFIS system is able to adequately and efficiently model the nonlinear behavior that a structure encounters when control devices, such as smart dampers or actuators, are installed in the structure. Having a system that can effectively predict the non-linear behavior allows for understanding of how the system will act, as well as being able to bypass the need for finite element models of the structure of interest. The WANFIS system is also an effective control algorithm to improve the performance of control system used on high-rise buildings and highway bridge structures, while also being able to reduce the number of sensors needed in a structure for feedback into the control device and reducing the computation time needed to determine the optimal control force in comparison with other control algorithms.

6. Recommendations and Future Work

Through the scope of this research and thesis, the wavelet-filtered adaptive neuro-fuzzy inference system model has been shown to be effective for use in system identification and structural control of structures. The system has been tested effectively for the system identification of a three-story building employing a smart, magnetorheological damper, and has been tested as an active control algorithm for an eight-story braced frame building and a highway girder bridge.

It is predicted that this system would be effective for various structures, and using it to look at a wide variety of structures would be desirable. This research could be expanded to validate this system for use in system identification and structural control of varying building heights, as well as testing it on a moment frame building. Also, studying different bridge structures, such as cable-stayed bridges or truss bridges, would provide further validity of the WANFIS system for structural control. To build upon the highway bridge model presented in this thesis, it would be interesting to look at a bridge with control devices located along the length of the bridge, as opposed to just the abutments. This could improve upon the performances provided in chapter 4 of this thesis, since the mid-span portion of a bridge that can be assumed to act as a simply-supported beam would have the largest responses, and the reduction of these responses at the mid-span point could improve the overall performance, essentially determining the ideal positions for control devices on a girder bridge.

7. References

Adeli H and Kim H 2004 "Wavelet-Hybrid Feedback-Least Mean Square Algorithm for Robust Control of Structures." *Journal of Structural Engineering*130.1 128.

Adeli H and Karim A 2000 “Fuzzy-wavelet RBFNN for Freeway Incident Detection.” *J. Trans. Eng.,* 126(6), 464-471.

Adeli H and Samant A 2000 “An adaptive conjugate gradient neural network-wavelet model for traffic incident detection.” *Comput. Aided Civ. Infrastruct. Eng.,* 15(4), 251-260.

Agrawal, Anil, Ping Tan, Satish Nagarajaiah, and Jian Zhang. "Benchmark Structural Control Problem for a Seismically Excited Highway Bridge-Part I: Phase I Problem Definition."*Structural Control and Health Monitoring* 16.5 (2009): 509-29. Print.

Ahlawat AS, and Ramaswamy A 2002 Multi objective optimal design of FLC driven hybrid mass damper for seismically excited structures. *Earthquake Engineering and Structural Dynamics* 31: 1459–1479.

Alhanafy T E 2007 "A systematic algorithm to construct neuro-fuzzy inference system". *16th International Conference on Software Engineering and Data Engineering*, p. 137.

Åström K J and Eykhoff P 1971 “System Identification-A Survey,” *Automatica*, 7(2): 123-162.

Bani-Hani K, Ghaboussi J. and Schneider SP 1999 Experimental Study of Identification and Control of Structures using Neural Network Part 1: Identification. *Earthquake Engineering and Structural Dynamics* 28(9): 995-1018.

Casciati, F., ed. 2003. *Proc., 3rd World Conf. on Structural Control*, Wiley, New York.

Catalao J P S, Pousinho H M I and Mendes V 2010 "Hybrid Wavelet-PSO-ANFIS Approach for Short-Term Wind Power Forecasting in Portugal." *IEEE Transactions on Sustainable Energy*.

Cha, Young-Jin, and Anil K. Agrawal. 2011 Decentralized Output Feedback Polynomial Control of Seismically Excited Structures Using Genetic Algorithm. *Structural Control and Health Monitoring*

Cha Y.J. and Kim Y. 2012a Comparative Study on Multi-objective Genetic Algorithms for Seismic Response Controls of Structures, *Structural Seismic Design Optimization and Earthquake Engineering: Formulation and Applications*, IGI Global, in press.

Cha, Y.J., Kim, Y., Raich, A., Agrawal, A.K. 2012b Multi-objective optimization for actuator and sensor layouts of actively controlled 3D buildings. *Journal of Vibration and Control,* In press.

Cha, Y.J., Agrawal, A.K., Kim, Y. and Raich, A. 2012c Multi-objective genetic algorithms for cost-effective distributions of actuators and sensors in large structures. *Expert Systems with Applications,* in press

Chen Y, Yang B Abraham A. and Peng L 2007 Automatic Design of Hierarchical Takagi-Sugeno Type Fuzzy Systems using Evolutionary Algorithms *IEEE Transactions on Fuzzy Systems* 15(3): 385-397.

Daubechies I 1992 *Ten lectures on wavelets,* Society for Industrial and Applied Mathematics, Philadelphia.

Du H. and Zhang N. 2008 Application of Evolving Takagi-Sugeno Fuzzy Model to Nonlinear System Identification. *Applied Soft Computing* 8(1): 676-686.

Faravelli L., and Spencer, B. F., Jr., eds. 2003. *Proc., Sensors and SmartStructures Technology,* Wiley, New York.

Faravelli L, Yao T 1996 Use of adaptive networks in fuzzy control of civil structures. *Microcomputer in Civil Engineering* 1996;12:67–76.

Filev DP 1991 Fuzzy Modeling of Complex Systems. *International Journal of Approximate Reasoning* 5(3): 281-290.

Gopalakrishnan K and Khaitan S K 2010 "Finite Element Based Adaptive Neuro-Fuzzy Inference Technique for Parameter Identification of Multi-Layered Transportation Structures." *Transport* 25.1: 58-65. Print.

Gu Z, and Oyadiji S 2008 Application of MR Damper in Structural Control Using ANFIS Method. *Computers & Structures* 86(3-5): 427-36

Guo H, Dong Z and Ma X. 2009 "WANFIS Model for Monthly Runoff Forecasting."*Hydroinformatics in Hydrology, Hydrogeology and Water Resources;*. Proc. of Symposium JS.4 at the Joint Convention of the International Association of Hydrological Sciences, IAHS and the International Association of Hydrogeologists, IAH, India. IAHS. 109-13. *Engineering Village*. Web. 16 June 2011.

Hashim SZ. Mohd and MO Tokhi 2004 ANFIS Active Vibration Control of Flexible Beam Structures. *Proceedings of the 7th Biennial Conference on Engineering Systems Design and Analysis* 1: 747-52.

Housner, G. W., Masri, S. F., and Chassiakos, A. G., eds. 1994. *Proc.,1st World Conf. on Structural Control.*

Housner, G. W., et al. 1997. ‘‘Structural control: Past, present and future.’’ *J. Eng. Mech.,* 123~9!, 897–971

Hung SL, Huang CS, Wen CM and Hsu YC 2003 Nonparametric Identification of a Building Structure from Experimental Data using Wavelet Neural Network. *Computer-Aided Civil and Infrastructure Engineering* 18(5): 356-368.

Hurlebaus S. and Gaul L 2006 Smart Structure Dynamics. *Mechanical Systems and Signal Processing* 20(2): 255-281.

Jalili-Kharaajoo M 2004 "Nonlinear system identification using ANFIS based on emotional learning". *Lecture notes in computer science (0302-9743)*, 3315, p.697.

Jang JSR 1993 ANFIS: Adaptive-network-based Fuzzy Inference System. *IEEE Transactions on Systems, Man and Cybernetics* 23.3: 665-85.

Jang J-SR, Sun CT and Mizutani E 1997 *Neuro-Fuzzy and Soft Computing.* Prentice Hall, Upper Saddle River, New Jersey, USA.

Johansen TA 1994 Fuzzy Model Based Control: Stability, Robustness, and Performance Issues *IEEE Transactions on Fuzzy Systems* 2(3): 221-234.

Johansen TA and Babuška R 2003 Multiobjective Identification of Takagi-Sugeno Fuzzy Models *IEEE Transactions on Fuzzy Systems* 11(6): 847-860.

Kareem, A., Kijewski, T., and Tamura, Y. 1999. ‘‘Mitigation of motions of tall buildings with specific examples of recent pplications.’’ *Wind Struct.,* 2~3, 201–251.

Karim A and Adeli H 2002a “Comparison of fuzzy-wavelet radial basis function neural network freeway incident detection model with California algorithm.” *J. Transp. Engineering.,* 128(1), 21-30.

Karim A and Adeli H 2002b “Incident detection algorithm using wavelet energy representation of traffic patterns.” *J. Transp. Engineering.,* 128(3), 232-242.

Kim, H.S. and Roschke, P.N. 2006 “Design of Fuzzy Logic Controller for Smart Base Isolation System Using Genetic Algorithm,” *Engineering Structures*, 28, pp. 84-96.

Kim, H.S. and Roschke, P.N. 2007, “GA-fuzzy Control of Smart Base Isolated Benchmark Building using Supervisory Control Technique,” *Advances in Engineering Software*, 38, pp. 453-465.

Kim Y. and Langari R 2007 Nonlinear Identification and Control of a Building Structure with a Magnetorheological Damper System. *American Control Conference*, New York, July 11-13, 2007.

Kim Y, Langari R. and Hurlebaus S. 2009a. Semiactive Nonlinear Control of a Building Using a Magnetorheological Damper System. *Mechanical Systems and Signal Processing* 23(2): 300-315.

Kim Y, Hurlebaus S, Sharifi R. and Langari R 2009b Nonlinear Identification of MIMO Smart Structures *ASME Dynamic Systems and Control Conference* Hollywood, California, Oct. 12-14.

Kim Y, Hurlebaus S., and Langari R. 2010a Control of a Seismically Excited Benchmark Building using Linear Matrix Inequality-based Semiactive Nonlinear Fuzzy Control. ASCE *Journal of Structural Engineering,* 136.

Kim Y, Langari R. and Hurlebaus S. 2010b Model-based Multi-input, Multi-output Supervisory Semiactive Nonlinear Fuzzy Controller. *Computer-Aided Civil and Infrastructure Engineering*, 25, 387-393.

Kim Y, Hurlebaus S, and Langari R 2011 Fuzzy Identification of Building-MR Damper System *International Journal of Intelligent and Fuzzy Systems*, in print.

Langari R 1999 Past, Present and Future of Fuzzy Control: A Case for Application of Fuzzy Logic in Hierarchical Control. *Proceedings*, *18th International Conference of the North American Fuzzy Information Processing Society-NAFIPS*, New York City, New York, USA, 760-765.

Lin, J.W and Betti R. 2004 On-line Identification and Damage Detection in Non-linear Structural Systems using a Variable Forgetting Factor Approach *Earthquake Engineering and Structural Dynamics*, 33(4): 419-444.

Nishitani, A., and Inoue, Y. 2001. ‘‘Overview of the application of active/semiactive control to building structures in Japan.’’ *EarthquakeEng. Struct. Dyn.,* 30, 1565–1574.

Ozbulut, O. E., Bitaraf, M., and Hurlebaus, S. 2011. “Adaptive control of base-isolated structures against near-field earthquakes using variable friction dampers.” Engineering Structures, 33, 3143-3154.

Ramallo JC, Yoshioka H and Spencer BFJr. 2004 A Two-step Identification Technique for Semiactive Control Systems. *Structural Control and Health Monitoring*, 11(4): 273-289.

Reda Taha MM, Noureldin A, Osman A and El-Sheimy N 2004 Introduction to the use of wavelet multi-resolution analysis for intelligent structural health monitoring. Canadian Journal of Civil Engineering,31(5), 719–731.

Reza S, Kim Y and Langari R 2010 Sensor Fault Isolation and Detection of Smart Structures. *Smart Materials and Structures* 19.10: 1-15.

Samant A and Adeli H 2000 "Feature extraction for traffic incident detection using wavelet transform and linear discriminant analysis." *Computer Aided Civil Infrastructure. Engineering.,* 15(4), 241-250.

Samant A and Adeli H 2001 "Enhancing neural network incident detection algorithms using wavelets." *Computer Aided Civil Infrastructure Engineering,* 16(4), 239-245.

Sharifi, R, Kim Y and Langari R 2010 Sensor Fault Isolation and Detection of Smart Structures. *Smart Materials and Structures* 19.10: 1-15.

Smyth AW, Masri SF, Chassiakos AG and Caughey TK 1999 On-line Parametric Identification of MDOF Nonlinear Hysteretic Systems. ASCE *Journal of Engineering Mechanics*, 125(2): 133-142.

Soong, T.T. 1990. *Active Structural Control: Theory and Practice*, Addison-Wesley Pub., New York.

Spencer, B.F. Jr., Suhardjo, J., and Sain, M.K. 1994. "Frequency Domain Optimal Control Strategies for a Seismic Protection." *J. Eng. Mech.*, 120(1), 135-158.

Spencer BF Jr, Dyke SJ, Sain MK and Carlson JD 1997 Phenomenological Model for Magnetorheological Dampers. ASCE *Journal of Engineering Mechanics* 123(3): 230-238.

Spencer, B.F. Jr., Christenson, R.E., and Dyke, S.J. 1999 Next Generation Benchmark Control Problem for Seismically Excited Buildings, in *Proceedings of the Second World Conference on Structural Control*, Kyoto, Japan, 2, 1351-1360.

Spencer, B.F.Jr. and Nagarajaiah, S. 2003 "State of the Art of Structural Control," ASCE Journal of Structural Engineering, 845-856

Takagi T and Sugeno M 1985 Fuzzy Identification of Systems and Its Applications to Modeling and Control. *IEEE Transactions on Systems, Man, and Cybernetics* 15(1): 116-132.

Thuillard Marc. *Wavelets in Soft Computing*. Singapore: World Scientific, 2001. Print.

Wang H 2010 "Hierarchical ANFIS Identification of Magneto-Rheological Dampers". *Applied mechanics and materials (1662-7482)*, 29-32 (1), p. 343.

Wang L and Langari R 1995 Decomposition Approach for Fuzzy Systems Identification. *Proceedings*, *the 34th IEEE Conference on Decision and Control*, New Orleans, LA, USA, 261-265.

Wu M and Adeli H 2001 "Wavelet-neural network model for automatic traffic incident detection." *Math. Comput. Applications,* 6(2), 85-96.

Yager RR and Filev DP 1993 Unified Structure and Parameter Identification of Fuzzy Models. *IEEE Transactions on Systems, Man, and Cybernetics* 23(4): 1198-1205.

Yan G and Zhou LL 2006 Integrated Fuzzy Logic and Genetic Algorithms for Multi-objective Control of Structures using MR Dampers. *Journal of Sound and Vibration* 296(1-2): 368-382.

Yang G, Spencer BF Jr, Carlson JD and Sain MK 2002 Large-scale MR Fluid Dampers: Modeling and Dynamic Performance Considerations. *Engineering Structures*, 24(3): 309-323.

Yang, J.N. 1982. “Control of Tall Building under Earthquake Excitation.” *J. Eng. Mech. Div.*, 108(EM5), 833-849.

Yang, J.N., Akbrapour, A., and Ghaemmaghami, P. 1987. “New Optimal Control Algorithms for Structural Control.” *J. Eng. Mech.*, 113(9), 1369-1386

Yang, JN, and Agrawal, AK 2002. ‘‘Semi-active hybrid control systems for nonlinear buildings against near-field earthquakes.’’ *Eng.Struct.*, 24~3, 271–280.

Yang, JN and Dyke, SJ 2003. ‘‘Kobori Panel Discussion: Future perspectives on structural control.’’ *Proc., 3rd World Conf. on Structural Control*, Wiley, New York, 279–286.

Yang YN and Lin S 2004 On-line Identification of Non-linear Hysteretic Structures using an Adaptive Tracking Technique. *International Journal of Non-Linear Mechanics*, 39(9): 1481-1491.

Yang, JN, Wu, JC, Kawashima, K., and Unjoh, S. 1995, ‘‘Hybrid control of seismic-excited bridge structures.’’ *Earthquake Eng. Struct. Dyn.*, 24~11, 1437–1451.

Yang YN and Lin S 2005 Identification of Parametric Variations of Structures based on Least Squares Estimation and Adaptive Tracking Technique. ASCE *Journal of Engineering Mechanics*, 131(3): 290-298.

Yen J and Langari R 1998 *Fuzzy Logic-Intelligence, Control, and Information*, Prentice Hall, Upper Saddle River, New Jersey, USA.

Zadeh LA 1965 Fuzzy Sets. *Information and Control*, 8(3): 338-353.